MDO with composite aeroelastic tailoring

Piyush Laxmikant Deshmukh

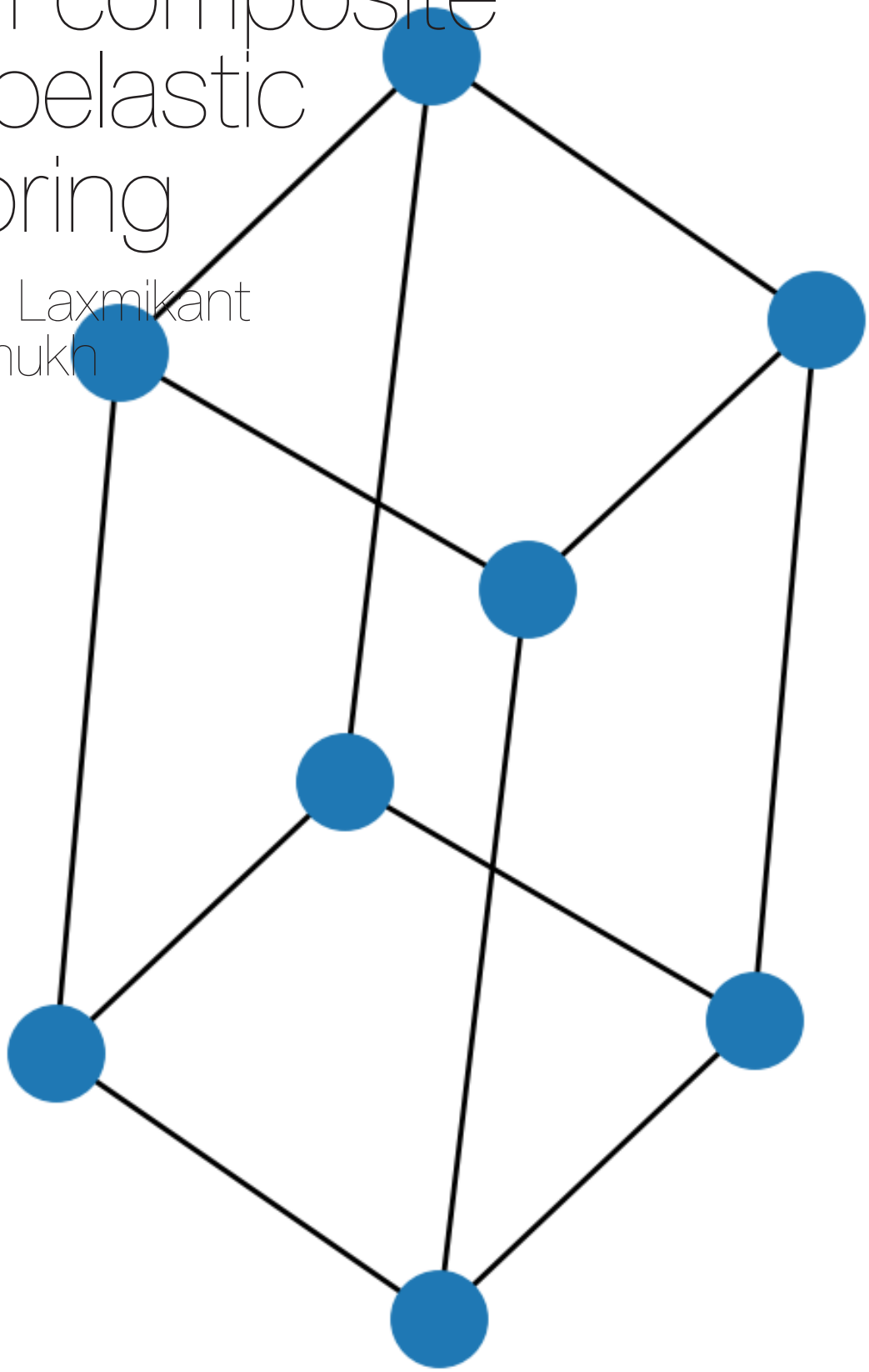

Technische Universiteit Delft

TU Delft

MDO with composite aeroelastic tailoring

by

Piyush Laxmikant Deshmukh

to obtain the degree of Master of Science
at the Delft University of Technology,
to be defended publicly on Monday August 31, 2020 at 13:00 hrs.

Student number:	4503031	
Project duration:	August 15, 2017 – August 31, 2020	
Thesis committee:	Prof. dr. ir. L.L.M. Veldhuis,	TU Delft
	Dr. Roeland De Breuker,	TU Delft
	Dr. Roelof Vos,	TU Delft

An electronic version of this thesis is available at `http://repository.tudelft.nl/`.

TU Delft

Acknowledgements

This Master thesis has truly been one of the toughest tasks I have undertaken until now and its significance lies beyond the technical outcomes. I am grateful to Prof. Roeland De Breuker for giving me the opportunity to perform my thesis at ASCM and also for his patience and positive enthusiasm. I am also grateful of my Phd supervisors, Imco van Gent and Darwin Rajpal for being so accommodating in dealing with my questions and guiding me when I was looking for a direction. Working with so many people has impressed upon me the importance of cooperation when trying to accomplish large tasks, something I will carry on in all my future endeavours.

I am thankful to Prof. Veldhuis and Prof. Vos for being a part of my graduation committee and accomodating of constraints.

I would also like to thank my friends Sumit, Shivang, Rishikesh and Harshil for making the tough course work memorable. I would also thank my roommates Pinakin and Saswat for helping to make the atmosphere light and cheerful through our deep conversations.

And finally, my parents and little brother have helped me to weather through my shortcomings and supported me by believing in me and thus instill the motivation to accomplish the thesis work. For this, I am forever indebted and thankful to them.

Piyush Laxmikant Deshmukh
Delft, August 2020

Preface

With the focus on the reduction of fossil fuel emissions, aircraft are continuously growing towards higher fuel efficiency. The traditional limits of aircraft performance can be surpassed through the use of composite materials which offer a reduction in aircraft weight. Due to the multidisciplinary nature of aircraft design, integration of different disciplinary analyses is required to arrive at a feasible design. The inclusion of composite design in the preliminary design process, however has become a challenge. This is due to the high computational cost associated with the composite aeroelastic tailoring tools used in the design process.

A possible solution is available in the form of surrogate models which can reduce the computational costs. The current work focuses on the development of a methodology that allows the inclusion of surrogate-based model in the optimization for a computationally expensive aeroelastic tool (PROTEUS) developed at TU Delft. The resulting methodology can be expanded to a generic, computationally expensive tool in a multidisciplinary optimization setting.

Wing design optimization is carried out based on surrogate modeling methodology and metal based design method. Comparison is made of the final optimized designs based on structural and performance parameters.

Contents

List of Figures

List of Tables

1

Introduction

The increased use of aircraft which work on fossil fuels also adds to environmental impact in terms of greens house gases, nitrogen oxides (NOx) water vapor, and particulate matter Schumann [63]. Reduction in the emission of these gases requires improvement in several aviation technologies.
The analysis of the Brequet Range Equation which is given in Greatrix [26] gives an overview of the various factors involved which can affect the aircraft performance in terms of the fuel consumption and efficiency of carrying weight represented by the payload. The equation has been represented in 1.1. The fuel consumption reduction can be made by a reduction in drag keeping the other factors constant. This can be controlled by the aerodynamics of the aircraft.

$$Aircraft\ Range = \frac{Velocity}{TSFC}\left(\frac{Lift}{Drag}\right)ln\left(1 + \frac{W_{fuel}}{W_{PL} + W_{OEW}}\right) \tag{1.1}$$

- $TSFC$ – Total specific fuel consumption
- W_{fuel} – Weight of fuel
- W_{PL} – Payload weight
- W_{OEW} – Operational empty weight

Additionally, the aircraft weight in the form of operational empty weight can be reduced by a reduction in the wing weight. The wing weight has a cascading effect on the overall aircraft weight. A lower wing weight leads to a lower overall aircraft weight. As a result the required lift reduces which is directly correlated to the induced drag. Hence, reduction in wing mass has a dual effect of reducing the actual aircraft mass and reduction in mass due to reduced fuel mass which is to be carried.

The application of composites has come up as a possible solution to reduce the weight of the aircraft structure. At the same time aeroelastic tailoring using composites enables additional freedom to the designer for adapting according to requirements posed by the loads encountered by the aircraft.

1.1. Composites and aeroelastic tailoring

Composite materials provide an advantage over traditional materials in terms of reduced wing weight Eastep et al. [15]. With the advent of composite material in the wing structure, an additional dimension was added to wing design. Composites can be used in several innovative ways to extract the required aeroelastic responses of the wing to enhance performance, some of which have been mentioned in Yu et al. [85]Stodieck et al. [69]. This ability is achieved by aeroelastic tailoring of the wing structure which couples the shape deformation of the wing to the aerodynamic loads in a manner that was not possible for traditional materials such as aluminum. An example can be seen in the form of bending and twist coupling of the wing. Additionally, the higher stiffness and strength to weight ratio of composites is the reason for the reduction in the wing weight while still carrying the required load Brooks et al. [3]. This allows for a higher aspect ratio due to the added strength to the wing structure. The aspect ratio has an inverse correlation with induced drag, thus an increase in the aspect ratio is beneficial for a

more fuel-efficient aircraft Brooks et al. [3]. Conversely, the aspect ratio has a proportional relation with wing weight. This indicates the trade-off which needs to be made between the wing weight and drag reduction to reach at an optimal wing design.

Review work of Jutte and Stanford [36] is used to gain a fundamental understanding of the application of aeroelastic tailoring, and the MDO studies where aeroelastic tailoring has been applied. Some of the papers with a fundamental exploration of aeroelastic tailoring are given in Shirk et al. [65]. The definition of aeroelastic tailoring as stated in by Shirk et al. [65] is given as "Aeroelastic tailoring is the embodiment of directional stiffness into an aircraft structural design to control aeroelastic deformation, static or dynamic in such a fashion as to affect the aerodynamic and structural performance of that aircraft beneficially."
To see the difference in aeroelastic response for different composite configurations the following Fig: 1.1 serves as a reference and gives an idea of the possibilities.

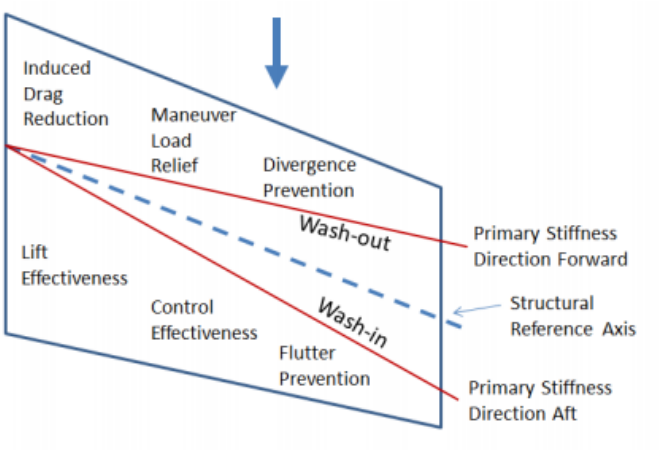

Figure 1.1: The effect that the location of the primary stiffness direction has on the characteristics of the wing Shirk et al. [65]

The application of composites in aeroelastic tailoring has been shown in the works of Weisshaar [79] and Eastep et al. [15].

With the growing interest in composite aeroelastic tailored wing, a new tool called PROTEUS was developed at TU Delft by Werter and De Breuker [80]. The tool is capable of performing structural optimization of a wing based on composite laminate parameters thus automating the process. Both static and dynamic aeroelasticity calculation capacity are present in the tool.

1.2. Multidisciplinary approach

The tight coupling between aerodynamics and structures due to the resulting flexibility of a high aspect ratio wing requires a multidisciplinary approach to wing design such as done by Gern et al. [21]. To attain the trade-off between the drag and wing weight as mentioned in the previous section. Due to the coupling, aero-structural studies were carried out Skoog and Brown [66].

Optimization studies could be carried out with resulting interactions which led to the growth of structural optimization. Additionally, due to more advanced analysis methods in individual disciplines other than structural analysis, it can be computationally challenging to execute such an optimization routine using a reasonable amount of time and resources. As the fidelity of the tool increases, the probability that the computational time will increase as well is high . Hence, the developments in data modeling in the form of surrogate models give a potential solution.
The major MDO studies performed have been listed in the table 1.1. The overview helps to determine which combination of disciplinary tools have been run in an optimization routine.

Certain studies also include acoustic analysis of the aircraft. The acoustic discipline has not been presented in the table 1.1. The indication from table 1.1 is that in a majority of the studies structural discipline involved in the analysis consider isotropic material such as aluminum. In the case of a study

Publication	Str [1]	Aero [2]	Fdyn [3]	control [4]	Perf [5]	Fin$_*$ [6]	Prop [7]
Peoples and Willcox [54]	✓	✓	✓			✓	
Perez et al. [56]	✓	✓	✓	✓	✓		
Jaeger et al. [34]	✓	✓			✓	✓	✓
Papageorgiou et al. [52]		✓	✓		✓		✓
Tzong et al. [73]	✓	✓					
Striz and Lee [70]	✓[8]	✓					
Wujek et al. [81]	✓	✓			✓		
Rao et al. [60]	✓	✓	✓	✓	✓		
Perez et al. [55]	✓	✓	✓				
Jones et al. [35]	✓	✓	✓	✓			
Suleman et al. [71]	✓	✓				✓	
Lambe et al. [41]	✓	✓					
Elham and van Tooren [16]	✓	✓					
Chiba et al. [5]	✓	✓					
Diedrich et al. [12]	✓	✓			✓		✓
Henson et al. [32]	✓[9]	✓					
Hwang and Ning [33]	✓	✓			✓		
Leifsson [43]	✓	✓	✓	✓	✓		✓
Morris [49]	✓	✓	✓	✓			✓
Wunderlich [83]	✓	✓					

Table 1.1: Multidisciplinary optimization (MDO) studies

involving composite design, the design variables are limited to the composite laminate design variables.

The exceptions are the two works employing the variation of the wing planform design variables in the works of Kennedy and Martins [38] and Wunderlich et al. [82]. While the works of Kennedy and Martins [38] considers swept-back wing, the work by Wunderlich et al. [82] considers a forward-swept wing.
There is hence a limited application of composite aeroelastic tailoring based on planform design variables to swept-back wings.

1.3. Computational expense

Implementation of composites in aircraft design proves as a popular option considering the motivations for major aircraft manufacturer's to shift towards more efficient aircraft. With the different disciplines involved however, application of computational studies to composites in multidisciplinary setting has been challenging. PROTEUS follows a similar trend and as a result has not been used in a multidisciplinary design application. One of the solutions is the application of surrogate modeling. The application of surrogate modeling in MDO has been demonstrated in the works of Kumano et al. [40] and Kanazaki et al. [37]. In the current case the PROTEUS tool presents such a challenge and hence the application of surrogate methods is intended in order to make the optimization routine feasible.

[1] Structure
[2] Aerodynamics
[3] Flight dynamics
[4] Flight controls
[5] Performance
[6] Financial
[7] Propulsion
[8] Composites are considered
[9] Composites are considered

2

Literature review

In order to conduct the study, the framework available is presented in the given section. The framework is based on two types of tools.

- Analysis tools
- Execution tools

Optimization studies are performed in a multidisciplinary approach that requires different analysis tools to be run in conjunction with each other. This facility is provided in the execution tools. The analysis tools on the other hand provide the physical models required to simulate the aircraft characteristics at various design points in optimization.

2.1. State of the art

Analysis tools

To evaluate the different designs, analysis has to be performed in terms of different disciplines. Depending on the problem, the disciplines can be increased or decreased as the designer wishes. The analysis employed by the tool may vary depending on the theory on which they are modeled. In the current case, the tools available at present are listed in table 2.1 along with a description of their function.

Analysis tools	
Tool name	Description
INITIATOR Elmendorp et al. [18]	Initiates an aircraft design based on top-level requirements
Q3D Mariens et al. [45]	Quasi 3D aerodynamic solver
EMWET Elham and van Tooren [17]	Wing mass estimation tool
PROTEUS Werter and De Breuker [80]	Aeroelastic wing analysis tool
PHALANX Pfeiffer et al. [57]	Flight dynamics tool

Table 2.1: Tools at TU Delft and their description

Since the initiator tool makes use of the top-level requirements, it is neglected. The primary interest in the current optimization is related to the planform design variables with a fixed top-level requirements. This is done by the selection of the D-150 aircraft configuration.

To get a better understanding of the internal workings of the analysis tools, further descriptions for the different tools is provided.

Werter and De Breuker [80] gives the overview for the PROTEUS tool. For the determination of aerodynamic loads the vortex lattice method is used. It is based on potential flow theory and thus assumes inviscid flow. This is sufficient for the purpose of load determination since the parasitic drag forces due to viscosity are much lower and hence are not instrumental in the calculation of aeroelastic

phenomenon. The tool makes use of lamination parameters for composite design. The advantage as presented in Dillinger [13] is that it reduces the number of design variables to define the composites arrangement compared to classical lamination theory which requires the angles, thickness and the sequence of the laminates.

Mariens et al. [45] presents Q3D which makes use of a combination of previously available programs (AVL Budziak [4], XFOIL Drela [14] and VGK Garabedian and Korn [20]) to reduce the computational effort required in the aerodynamic analysis. For inviscid analysis the AVL software is implemented which is based on the vortex lattice method. This makes use of potential flow solutions to determine the lit coefficient and induced drag of the aircraft. For the viscous case, Q3D makes use of the tools xfoil and VGK programs. The program makes use of the xfoil and avl for low subsonic analysis while switching to VGK for the transonic analysis. The results have been tested with an established software, the MATRICS-V van der Wees et al. [74] to confirm that the accuracy of the tool is as required. The tool can be used for load determination and drag calculation. The drag force can be categorized into profile drag and induced drag. While the profile drag is a further combination of skin friction drag and pressure drag. The effect of sweep is included in the results and can be accounted for in the drag force.

The capabilities of Q3D for drag and load analysis prove an asset for the case of wing design optimization. The application of the tool has been demonstrated with an example by the authors in Mariens et al. [45]. The reduced computational time is also an advantage.

Elham and van Tooren [17] presents EMWET as a weight estimation tool that works in two steps. The first step is to perform a weight estimation of the wing by assuming a box structure. In the second step, the tool calculates stress by using the aerodynamic load data on the finite element model of the wing. Since the wing weight required is dependent on the structure, when it is subjected to loads, a new structure is required to sustain the stresses. Thus a coupled system occurs which requires consistency to have an equilibrium between the two disciplines. It was developed to perform quick weight estimation in multidisciplinary optimization and thus is useful in the current study.

Pfeiffer et al. [57] describes phalanx as a flight dynamics assessment code. It combines results obtained using the aerodynamics, structures, propulsion to create a non-linear flight dynamics model. The tool can be applied for aircraft flexibility during maneuvers, morphing aerostructures, landing gear models, etc. The paper also discusses the creation of a CPACS wrapper for a new tool. (In this case, CPACS represents a format of representing data. It makes it easier to exchange information between different tools. Further details on CPACS are given in execution tools). The CPACS wrapper acts as an interface between the tool and the CPACS file since the form of inputs required for the tool are different for each tool compared to the standardized format used by the CPACS. It also suggests that in case the tool fidelity levels are separate it is beneficial to have separate CPACS wrappers codes. It suggests future possible work to be done in terms of finding the best possible strategy for integrating the tool using CPACS. Tool chain is still to be validated. Additionally, the effect of individual tool accuracy on the complete workflow is also to be studied.

Execution tools

The high interdisciplinary nature and collaboration required in new aircraft designs propelled the Agile program which is a consortium of several aerospace institutes, research centers, and industry Ciampa and Nagel [7]. The aim was to develop MDO processes that could significantly reduce aircraft development time. The overall program worked in several steps, each increasing in design complexity,accuracy and reliability. As is the approach in multidisciplinary optimization problems the understanding of the state of the art can be obtained by decomposing the various aspects of the process. With increasing development in software and automation, dedicated programs and systems have been developed for MDO. The developments have been mentioned in the knowledge architecture and collaborative architecture papers van Gent et al. [75]Ciampa et al. [8].
With the aim of the application of MDO technologies, there have been several new developments within the AGILE framework. The development aims to reduce the time for aircraft design and development as well as develop more efficient aircrafts [6]. Some of the advances in design methodologies which formed a part of the framework are given below.

CPACS

In order to support MDO one of the concepts which emerged was CPACS (Common Parametric Aircraft Configuration Schema) Nagel et al. [50]. This was a result of the effort at DLR (Deutsches Zentrum für Luft- und Raumfahrt) to create a standard data file for the aircraft which could be used by different disciplines thus reducing the number of interfaces. Some understanding of the functioning of a common language can be gained from figure 2.1.

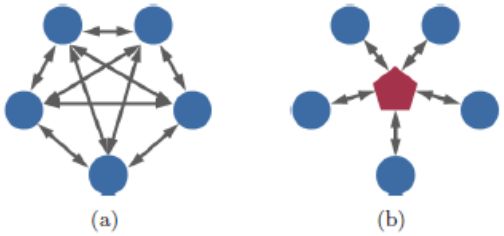

Figure 2.1: Overview of CPACS exchange a) without a common standard increasing the number of interfaces, b) With a common standard and reduced number of interfaces Rizzi et al. [61]

CMDOWS

In an MDO problem, the disciplinary tools, exchanged data and process connections keep evolving until the formulation is complete van Gent et al. [76]. CMDOWS is a file to store the MDO formulation in a neutral format. It shows similarities with CPACS. While CPACS defines the standard format of the aircraft data, CMDOWS takes care of the process data to define the workflow .

OPENMDAO

OpenMDAO Gray et al. [24] is an open-source integration platform for the various tools and creates the final process for optimization. The details regarding interacting with and working on the openMDAO environment are given in Gray et al. [25]. Case studies for design applications have been given in Gray [23] and Hendricks [31]. In the current case openMDAO is chosen as the integration environment.

2.1.1. Multidisciplinary Optimization (MDO)

The application of optimization has roots in aircraft structural studies. It started with applications in structural optimization. Following the idea of structural optimization, multidisciplinary optimization developed which considered not only structural but aerodynamic and performance evaluations. Since the design of an aircraft works at the confluence of several disciplines, MDO developed as a means for new aircraft designs which could work with several requirements simultaneously and deliver the best design possible for the requirement Sobieszczanski-Sobieski and Haftka [67].

The different approaches can be categorized for reference. The work of Martins and Lambe [47] gives a comprehensive overview of the different MDO architectures. In order to decide on the architecture, in the current case, the capability of KADMOS plays a role in the decision making. KADMOS is a tool developed at TU Delft which aids in formulating an MDO problem. It is based on graph theory which was used to show that the method could be used in MDO formulation by Pate et al. [53]. The size of the MDO problem has been mentioned as a bottleneck in van Gent et al. [77]. Size, in this case, refers to the number of analytic tools and variables which are involved in the MDO problem. Besides the actual run-time of the MDO problem, setting up the problem with the required interlinks is a difficult task. In order to reduce the efforts required for this formulation, KADMOS was developed. Besides faster formulation, the objectives of KADMOS are several. With traditional methods, once the MDO problem was structured using a particular architecture, it was not possible to manipulate the achieved result to construct a different MDO architecture. KADMOS provides this capability and thus several methods can be formulated and tested with reduced setup time. This agility is also present in terms of the number of tools which can be selected, thus the number of disciplinary analysis to be performed can be increased. The details regarding the working of the KADMOS are given in van Gent et al. [77]. Figure 2.2 gives an understanding of the MDO process and the role of MDO formulation.

It shows that the use of MDO has become highly essential in aircraft design. However, in order to produce the workflow, the difficulties of joining the tools together in the different architectures have

been made easy by the use of KADMOS which reduces problem formulation time. KADMOS has also made it possible to alternate between multiple architectures giving a more common baseline to compare the architecture performances than the traditional formulation.

Martins and Lambe [47] present the different architectures in a standard format. The differences in the architectures can be seen based on the constraints and consistency requirements in the MDO architectures. The MDF architecture has minimum number of state variables exchanged between the disciplines whereas the all-at-once solution has the highest number of state variables exchanged between the analysis tools. The architectures on a top level can be divided as monolithic and distributed. In case of monolithic architecture the optimizer evaluates the design at each converged design point. In case of distributed architectures the optimization function is combined with the analysis evaluation blocks and hence the optimizer receives variables even if a consistent design point has not been reached.

Tedford and Martins [72] present a study in the comparison of different architectures using the pyMDO platform which performs a function similar to KADMOS in MDO formulation. Hence, it allowed the authors to use a baseline problem and apply it in different MDO methods. The authors provided quantitative metrics for comparison. The work gives a framework to use a common MDO problem and its relation to the performance of the MDO algorithm. The presented approach uses the number of local variables and number of design variables for comparison. It was found that MDF and IDF architectures to be more robust and had ability to deal with different problem formulations whereas the architectures which made use of approximate functions were more dependent on the problem. The use of complex step derivatives and finite differences is made to calculate the derivatives required to drive the search algorithm. The results could be expectantly different for the case of adjoint based sensitivities.

The study serves to show the probable application of KADMOS in MDO architecture studies. The metrics used in this paper for architecture performance comparison can be used.

Martins and Hwang [46] In the calculation of the sensitivities, which refers to the derivatives of the objective and constraints with respect to the design variables, different methods available were presented and unified under a common framework. A result on the effect on relative error of the finite difference method and complex step shows that the reduction of step size can also have a negative effect on the relative error in case of finite difference.

The mathematical framework for optimization is gathered from the bookSobieszczanski-Sobieski et al. [68]. The derivatives and search step thus together help to incrementally move towards an optimum. The various ways of calculating the derivatives have been mentioned previously. It presents the two fundamental optimization algorithms, gradient based and randomized optimization such as genetic algorithm. One of the conclusion was that the randomized algorithm tend to be more expensive compared to the gradient based algorithms. There is no universal approach in selection of an optimization algorithm and it varies with the problem to be solved.

Thus the use of gradient based and non-gradient based optimization methods can be tried to check the efficiency of the MDO strategy for the two different methods. Thus the optimization algorithm has an influence on the number of computation performed before converge is reached. The greater amount of time in randomized algorithm is compensated by the fact that randomized algorithm are more robust and can traverse over a more varied design space than a gradient based algorithm.

MDO requires evaluation from several analysis tools. With advances in each individual discipline, the computational requirements of the tools have increased as more complex analysis can be performed with higher accuracy. There is a continuous attempt to offset the computational time. Han and Zhang [30]Zhang et al. [86].To reduce the computational expense, an alternative in the form of meta-modelling or surrogate models is a possibility suggested in literature as has been applied in [42]. Additional review regarding the details of surrogate methods is discussed in section 2.1.2.

2.1.2. Design of experiments and surrogate modelling

As presented briefly in the section on multidisciplinary optimization the application of surrogate models helps in reducing the computational time by replacing the physics-based tool with a mathematical model. The advantage of faster function evaluations is that it makes sensitivity and design studies feasible Queipo et al. [58]. There are different possibilities for working with surrogate models. A review on surrogate-based optimization is provided in Wang and Shan [78],Yondo et al. [84]. They give an under-

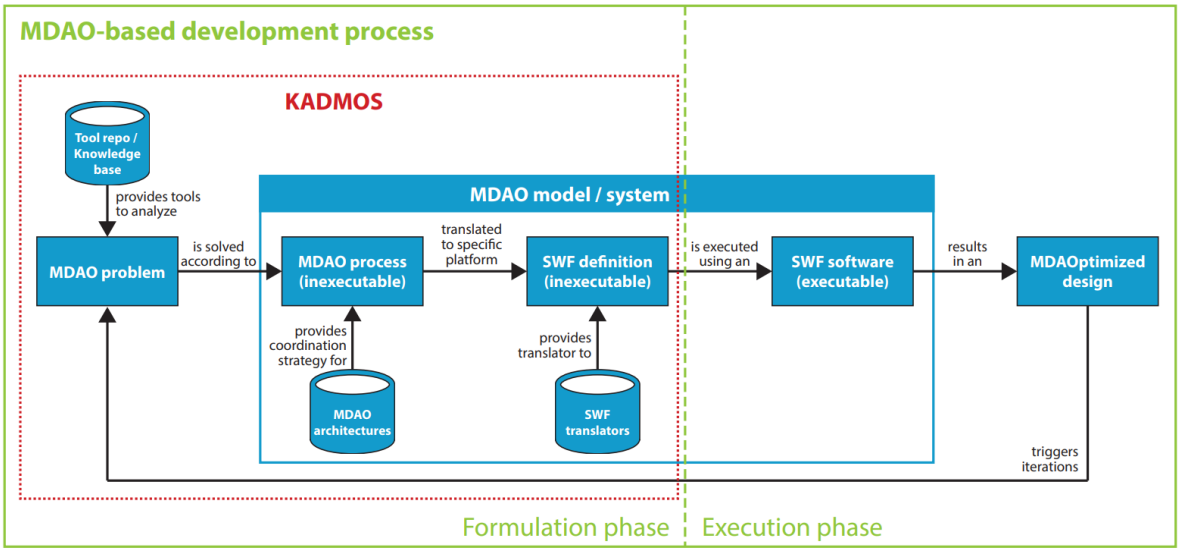

Figure 2.2: Overview of executing a MDO problem from formulation to running the simulation. The process is divided in two phases: formulation (left) and execution (right). The part simplified by KADMOS is marked by the red box. Figure 1 from van Gent et al. [77]

standing of the concepts which are involved in the surrogate optimization and the practical implications of the methods which are useful for implementation. Evaluation strategies are also presented for how well a surrogate model works. The various design of experiments used in the previous studies among aircraft design involve the use of latin hypercube sampling. According to Yondo et al. [84] with a limited computational budget, the optimal use between the low fidelity model obtained from data and the high fidelity model which uses physics-based equations is required. The idea being that integrating a hybrid model which modifies the surrogate model based on the accuracy levels required is more effective. It selects among the physics-based and surrogate model. At regions of high errors for the surrogate method, the model switches to physics-based tool. This creates an additional requirement to decide between the use of a hybrid model and a sole surrogate model.

Given the bias and variance errors, a suitable cross validation strategy is suggested in [22] called the k-fold cross validation method. The models are constructed and tested on all the available points. This is done by first dividing the design space into n sections. Using the n-1 groups, the surrogate is constructed and the prediction accuracy on the remaining set is checked. This is repeated for the entire collection of points thus allowing to use all available points.

It can be concluded that the use of aeroelastic studies use the traditional wing and thus there is a lack of studies which makes use of aeroelastic tailoring for MDO studies. The disciplines in the table 1.1 are used as a measure of the kind of MDO studies to be performed and also to help selection in the tools which are available at the faculty. These tools and their capacities are discussed in the next section.

2.2. Research questions

The structure of the problem can be visualized in a mind map given in Figure 2.3. The limited inclusion of composite aeroelastic tailoring in the MDO process thus gives us the core research question.

To develop a multidisciplinary optimization work flow with the inclusion of composite aeroelastic tailoring using surrogate modeling techniques.

The challenge presented by the computational time of PROTEUS forms an implicit challenge in the research question. The sub questions which can be formed to answer the research question are as follows

1. What is an efficient method to include surrogate model of PROTEUS in the MDO problem?

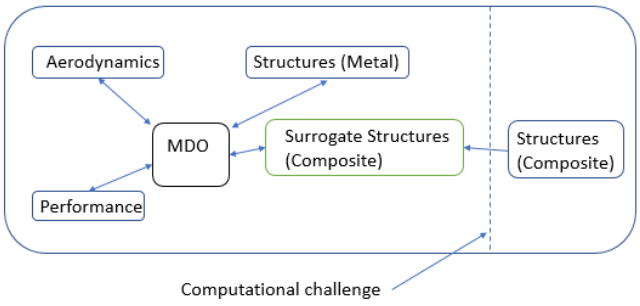

Figure 2.3: Disciplines in MDO with the computational barrier in case of aeroelastic tailoring

2. Upon the inclusion of PROTEUS in MDO, what are resulting effects on the wing design?

2.3. Methodology

Before the PROTEUS tool can be integrated into the MDO work-flow, a design of experiments and a subsequent surrogate modeling of the results is to be performed. This surrogate model is a representative of the actual model. The surrogate model obtained is evaluated for accuracy. This validation helps to gain confidence in the surrogate model.The k-fold validation method described previously will be used for this purpose. Subsequently, the PROTEUS surrogate will be implemented in the MDO work-flow which brings to the step of preparing the MDO work-flow.

While the inclusion of PROTEUS surrogate allows for a composite wing to be designed, a secondary method is also formulated. In this second scenario the initial optimization is performed using the traditional metal based weight estimation tool EMWET. The optimized planform is subsequently used as an input to PROTEUS to produce the optimized composite structure. A graphical representation of the methodology with the inclusion of PROTEUS along with the secondary method is given in Figure 2.4 while the steps to create the executable file is shown in figure 2.5.

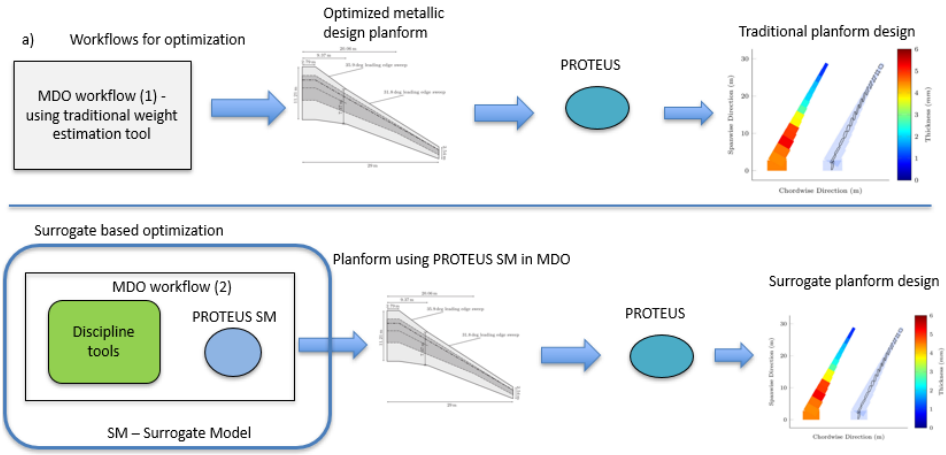

Figure 2.4: A comparison between the two methodologies proposed for composite wing design with variation in planform design variables

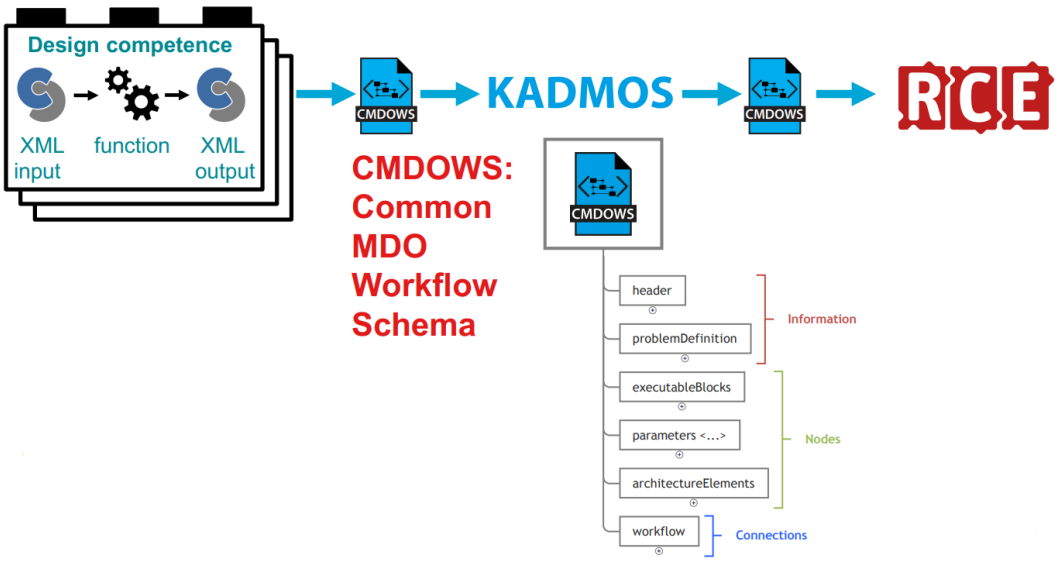

Figure 2.5: Execution overview for the MDO workflow. Taken from de Vries et al. [10]

3

Surrogate modeling

With the requirement of reduction in the computational time of the tools, a suitable method to implement surrogate functions of the involved tools is required. With this motivation in mind, the current section gives the understanding of the tool KADMOS and the development which were added to support surrogate creation within KADMOS.

The KADMOS graph generation methodology is described in the work of van Gent et al. [77]. The work of Pate et al. [53] serves as a reference in the use of graph-based descriptions of MDO workflow. Based on the preliminary ideas in Pate et al. [53] and the open-source graph theory library NetworkX, an automatic MDO formulation program is developed which is KADMOS. KADMOS forms a part of the AGILE development program which aims to simplify the creation and execution of MDO workflow and allow for a greater number of design studies than are possible by the traditional methods.

The working of KADMOS deals with the manipulations of digraphs which are a subcategory of graphs. To get a simple understanding of the graphs and some of the ideas involved a basic overview of what is meant by the KADMOS graph is given in the next section.

3.1. Kadmos Graph

A graph can be described by nodes and edges as shown in figure 3.1. Mathematically, a graph can be described as $G = (V, E)$ where, V is the set of vertices and E is the set of edges. Additionally, the condition $E \subseteq [V]^2$ is satisfied which implies that the two elements within the edge, are a 2 element subset of vertices. With the nodes and edges defined, additional attributes can be added to the nodes or edges.

Function role : One commonly used attribute is the function roles which is divided into the following five categories.

1. Pre-coupling
2. Coupled
3. Post-coupling

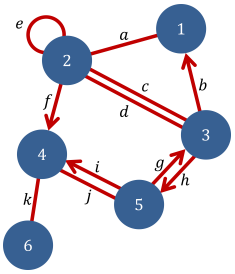

Figure 3.1: A general graph (Win [1])

4. Pre-desvars
5. Post-desvars

This division is used for the function nodes which represent the individual analysis tools. The problem roles help to categorize the function nodes and thus simplify the analysis. Similarly, the vertices can also be separated as function nodes and variable nodes with the direction of the edge describing the relation of the variable with respect to the function. The edges can be of several types however, in the case of KADMOS since the graphs have to be digraphs, the edges are limited to being unidirectional which would be similar to edges b,g and h to name a few in the figure 3.1.
As KADMOS makes use of NetworkX Hagberg et al. [29] library of python, the NetworkX library on github has a general description for the graphs NetworkX manipulates. The graphs used in KADMOS have uni-direction edges, these fall under the category of digraphs and the methods applicable to digraphs are also applicable to KADMOS graphs.
Cyclic Graph : An additional property of the KADMOS graphs which needs to be known is the occurrence of cycles. In a cyclic graph, it is possible to travel along the direction of the edges to form a cycle that has the same starting and endpoints. Depending on the various paths possible, each individual path is identified as a cycle.

3.2. Surrogate models

The creation of surrogate model is based on the input and output of the particular available method. The general surrogate modeling methodology can be seen in figure 3.2. The simulation based model (f) generates the data f_1. This data is used to create the estimated model ($\hat{f}$) which can be used as replacement in the optimization runs.

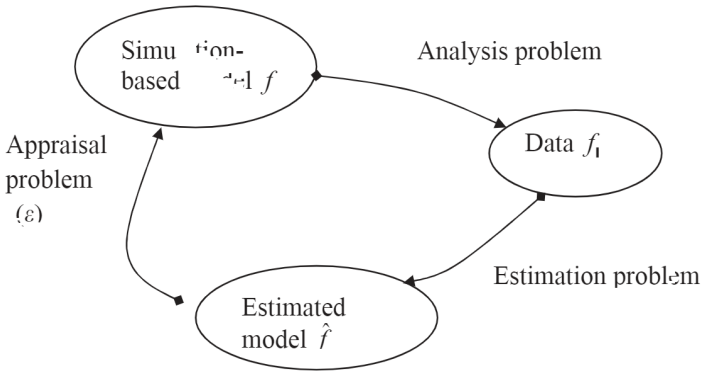

Figure 3.2: The relation of the existing model to the surrogate model Queipo et al. [59]

In order to create the estimated model, several mathematical functions have been presented in the literature. Some of the standard methods which can be used for estimation have been presented in Forrester and Keane [19].
Kriging: From among the available methods, kriging is a popular method used for surrogate creation in aerospace and hence the current work focuses on the kriging method. In a future pursuit, the other methods can also be tested for their performance against the kriging results presented in this work.

The estimated inputs for a particular solution are those variables which need to be supplied as inputs for running the DOE workflow. The corresponding output is then modeled with respect to the estimated inputs.

3.3. Optimum graph for surrogate

KADMOS deals with the formulation phase of the MDO problem while the execution is done using the OpenMDAO Gray et al. [25] tool. OpenLEGO de Vries [9] forms the link between the formulation phase and the execution phase. In the creation of KADMOS output, the Fundamental Problem Graph (FPG) obtained displays the interconnections of the various tools. It represents the optimization problem in a graph form. Thus, the overall MDO problem is represented in the form of an FPG where we get an

overview of the various dependencies of the functions. These dependencies can be used to reduce the computational cost. The steps in graph manipulation in KADMOS are understood through figure 3.3 which form the formulation sub-part of the overall optimization workflow.

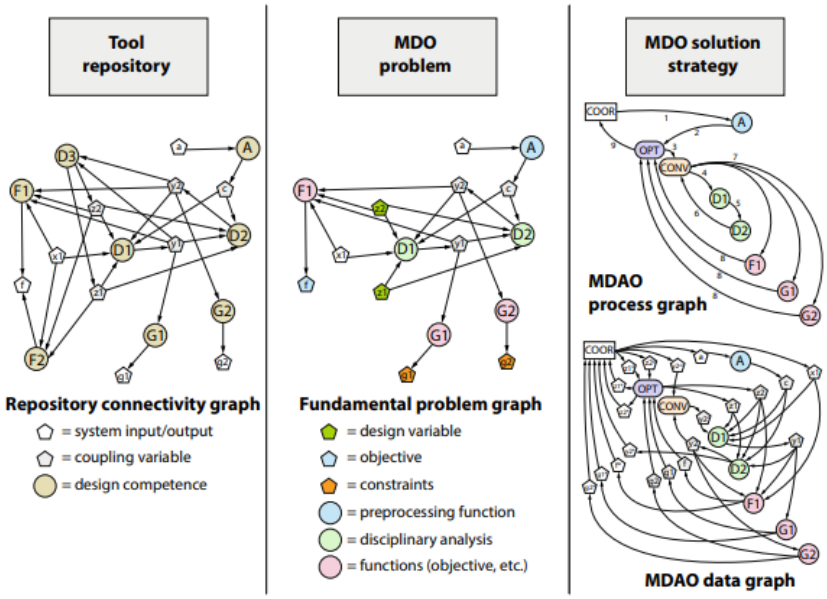

Figure 3.3: The formulation strategy in KADMOS (with the use of the sellar problemSellar et al. [64]) Aigner et al. [2]

The development of surrogate models requires the use of the design of experiments methods where the number of input variables determines the number of function execution. In the current case, the number of function evaluations required is determined to be at 10. Hence, the cost of generating the data for surrogate function can be expressed as

$$Totalruntime = 10 n_e t_r \tag{3.1}$$

where n_e is the number of estimated inputs and t_r is the run time for the function. The runtime can thus be reduced by decreasing the number of estimated inputs.

In the creation of the surrogate function an optimum graph can be used which helps to reduce the number of runs that are required to build the surrogate model. An example can be described in the figure 3.4 given below. For the function D3, the number of inputs is quite high. With the addition of the function D2 a surrogate of the combined functions, D3 and D2 can be created. This combined function has a lower number of estimated inputs. Thus, the idea which forms the base for the optimum graph is that the computational cost to build the surrogate function can be reduced by combining functions together and creating a surrogate for the combined functions.

In order to make the selection of the functions to be run together with the target surrogate function, four algorithms were hence developed.

1. Brute-force
2. Function combinations
3. Topological method
4. Adjacency method

One of the primary parts of the algorithm is a command available within KADMOS for function sequencing in FPG. The specific sequencing command applied in KADMOS is the single-swap. The sequencing arranges the function in a manner that reduces the number of feedback inputs required. Example of feedback are variables s4 and s in fig 3.4.

The details for the different algorithms are given below:

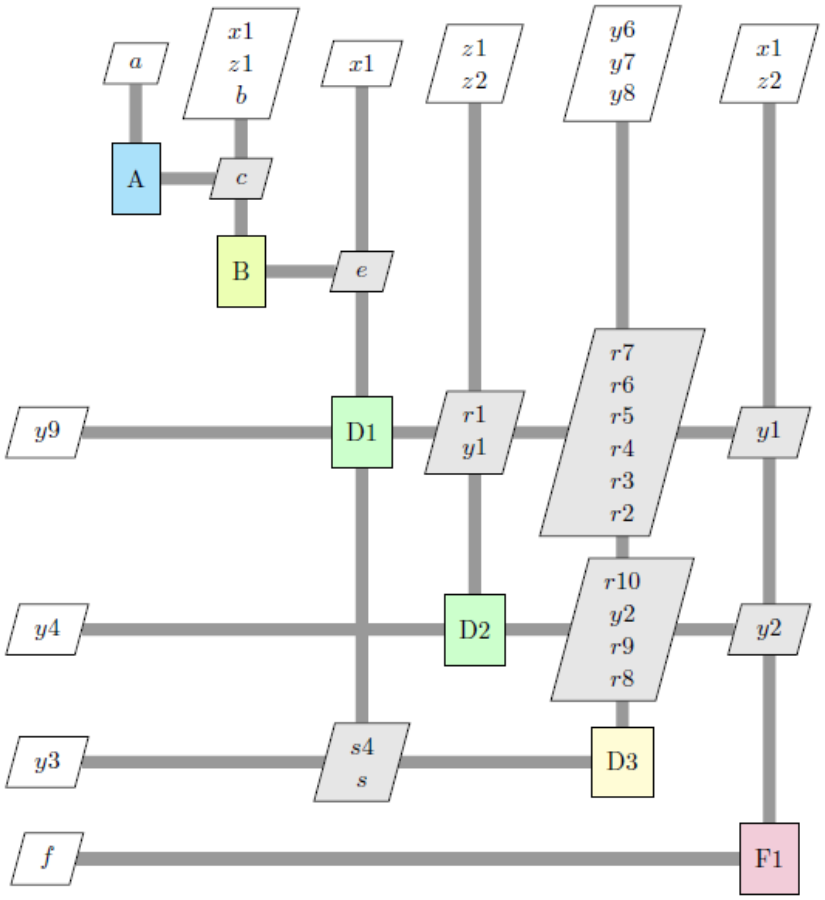

Figure 3.4: Validation case

3.3.1. Brute-force

Brute-force algorithm is the most basic approach which traverses through all the possible sub-graphs which includes the target surrogate function. The order of the functions in the sub-graph is also determined through permutation. The valid solutions are filtered from the total possible solutions. To identify a valid solution, the target surrogate function needs to present in the sub-graph obtained. In order to reduce the computational effort an additional filter is added which categorises the target surrogate function based on its functional role.

Since the brute force method is extensive in its search for solutions, it serves as a benchmark against which the other algorithms can be checked further on.

3.3.2. Function combinations

The brute force method while accurate had a low computational limit where it could handle a graph with very few functions. This is since the time required would scale proportional to the factorial of the number of functions. A second alternative method was thus implemented based on the combinations of the various functions in the graph. The computational time for this algorithm scaled exponentially as opposed to the brute force method which scaled in a factorial manner. Thus the limit of the number of functions was increased. The algorithm implemented is thus presented below.

3.3.3. Topological method

While the combination method provides a faster method, it has a limited application since the computational effort rises exponentially with the number of functions in the MDO problem. The topological method is based on the topological sort algorithm presented in [39] and can be applied to a larger function group than the combination method. A requirement for the application of the command all_topological_sorts from NetworkX is that the input graph has to be a directed acyclic graph (DAG).

Algorithm 1 Brute force

```
Get function order
Remove post-coupled functions
Find the function category
if Function category = pre-coupling then
    Remove post-coupling and coupled functions
    Create permutations of the functions
    if Target function in permutation then
        if Function not linked to target function then
            Remove function
        end if
    end if
    Evaluate the function sub graphs obtained
    Return estimated inputs, run times and function orders
end if
if function category = coupled then
    Remove post-coupling function
    Repeat steps 6 - 13
end if
```

Algorithm 2 Fuction combinations

```
Get dependent functions
Find the target function category
if Function category = pre-coupling then
    Get main sub-graph with dependent functions and target function
    Apply topological sort to main sub-graph to obtain topological function order
    for Each combination in function combinations do
        Get sub-graph for function combination
        for Function in sub-graph do
            if Function not linked to target function then
                Discard combination
            else
                Arrange functions according to topological function order
                Evaluate the function sub graphs obtained
                Return estimated inputs, run times and function orders
            end if
        end for
    end for
end if
if Function category = coupled then
    Get sub-graph with dependent functions
    Get function combinations
    for Combination in function combinations do
        if Function not linked to target function then
            Discard combination
        else
            Arrange functions through single-swap function order for minimum feedback
            Evaluate the function sub graphs obtained
            Return estimated inputs, run times and function orders
        end if
    end for
end if
```

Thus, the feedback couplings in the graph are removed before applying the all_topological_sort com-

mand. The solutions obtained by topological sort were sensitive to the density of the graph and the

Algorithm 3 Topological method

```
Get dependent functions
Create sub-graph based on dependent functions
Get function graph from sub-graph
Get variable coupling dictionary
Build source and target dictionary of functions
Find the function category
if function category = pre-coupling then
    Reverse edge directions
    Apply branching to the directed acyclic graph
    Reverse edge directions
    Get zero in-degree nodes
    if Zero in-degree nodes < 8 then
        Apply all topological sorts
        Evaluate the function sub graphs obtained
        Return estimated inputs, run times and function
    else
        Solution not possible, too many in-degree nodes
    end if
end if
if function category = coupled then
    Get best possible function order with single-swap ( minimum feedback is calculated based on number of unique variables in feedback)
    Remove feedback edges of sub-graph to create DAG (directed acyclic graph)
    Remove functions not a source of target function
    Repeat steps
end if
```

location of the function within the graph structure, thus, the method was unreliable although effective for some cases.

3.3.4. Adjacency method

The major task in the four algorithms is to find a sub-set graph of the complete graph. While this graph has to be evaluated based on the number of estimated inputs and the total run-time to calculate the objective. In the adjacency method, to find these connected subsets, an algorithm developed by Luo et al. [44] has been used through a modification. The original algorithm is developed for an undirected graph to find all the possible connected subsets given a root function, which in the current case would be the target function. The KADMOS graphs are directed hence the algorithm had to be modified to function for direct graphs as inputs. The computational cost for the algorithm is proportional to the square of the number of functions which makes it suitable for cases with large number of disciplines. The pseudo-algorithm for the method is given below.

3.4. Algorithm testing

Validation and verification tests are performed on the algorithms developed which have been presented in this section. Finally, the ability of the algorithms to scale up is also shown, in the performance evaluation. The scaling up ability indicates the limits of the various algorithms developed in terms of the time required to evaluate.

3.4.1. Validation

The application of the various algorithms is tested though the case presented in figure 3.4. The problem setup is as follows:

- A,B, D1, D2, D3 and F represent function blocks.

Algorithm 4 Adjacency-method

1: Get dependent functions
2: Create sub-graph based on dependent functions
3: Get function graph from sub-graph
4: Find the function category
5: **if** function category = pre-coupling **then**
6: Set initial values
7: $G = Functiongraph$
8: $R, Vcap = surrogatefunction$
9: Run $FindConnectedSubsets$ routine with the initial values
10: Reorder connected subsets using topological order of function graph
11: Evaluate the function sub graphs obtained from the connected subsets
12: Return estimated inputs, run times and function orders
13: **end if**
14: **if** function category = coupled **then**
15: Get best possible function order with minimum feedback (minimum feedback is calculated based on number of unique variables in feedback)
16: Remove functions after surrogate function in function order
17: Remove feedback edges to create DAG
18: Create function graph
19: repeat steps $6 - 11$
20: Return estimated inputs, run times and function orders
21: **end if**

- D3 represents the target function block.
- The variables x1, z1 and z2 are the design variables.
- Variables a, b, y6, y7 and y8 represent non-variable function inputs. These are considered constant.
- The variables y9, y4, y3 and f are individual function outputs.
- The rest of the variables are referred to as the coupling variables. These are exchanged between the different functions.
- Lastly, the variables s4 and s, while being coupling variables, are also feedback variables.

The brute force optimum solution is given in figure 3.7. The number of coupling inputs to the function D3 is ten. For the sub-graph which can be used to build a surrogate of D3, the number of estimated inputs is reduced to 5. To calculate the objective value the run times of the individual functions are used which are given in table 3.1.

Table 3.1: Run times of the functions in the validation case

Function	Run time
A	2
B	4
D1	10
D2	20
D3	100

The objective value for the best solution can be calculated as

$$obj = 10 * estimated\ inputs * \ total\ runtime \tag{3.2}$$

which comes out to be 6800, the value obtained in the figure 3.7 for the best solution.

The adjacency method makes use of modification within a previously available algorithm. The validation is thus done in 2 parts. First, the modified adjacency method is checked for the accuracy on a directed graph since it was originally designed for an undirected graph. This is followed up with the test on the sample case on which all the algorithms are validated.

Two test cases for the directed graph adjacency algorithm are shown in figures 3.5 and 3.6. The set of solutions which are obtained for case 1 are given below represent the exhaustive set of solutions for this case.

- (5)
- (4, 5)
- (3, 4, 5)
- (4, 5, 7)
- (8, 4, 5, 7)
- (8, 9, 4, 5, 7)
- (3, 4, 5, 7)
- (8, 3, 4, 5, 7)
- (3, 4, 5, 7, 8, 9)

For case 2, from among the solutions obtained, the case [5,4,10,3,8] is neglected as is expected of the modified algorithm. This is since the modified algorithm can only traverse in a direction which is opposite to the direction of the edge.

The two cases hence display the validity of the modified connected subset function used in the adjacency algorithm.

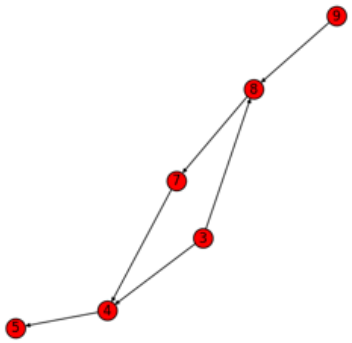

Figure 3.5: Adjacency algorithm modification to find connected subsets for directed graphs (case 1)

3.4.2. Verification

Brute force solution serves as a basis for verification of the results obtained from the combination, topological sort and adjacency methods. In table 3.2 the comparison is done for the case of problems consisting of up to 8 disciplinary tools. The variable complexity script created previously has been used for generating cases based on a varying number of connections between the function nodes.

In a successful evaluation, the method is able to find the best possible solution which has also been determined by the brute force method. In certain cases, the methods are unable to give the best possible solution and are hence counted as the error cases. In the unresolved cases, the computational time of the method exceeds beyond 300 seconds and hence there is no valid solution obtained in such cases.

The results indicate that while the topological method is promising, the reliability of the adjacency method is higher making it a more suitable algorithm.

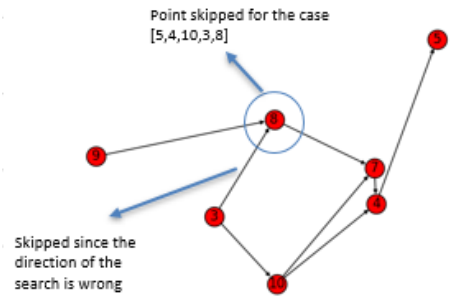

Figure 3.6: Adjacency algorithm modification to find connected subsets for directed graphs (case 2)

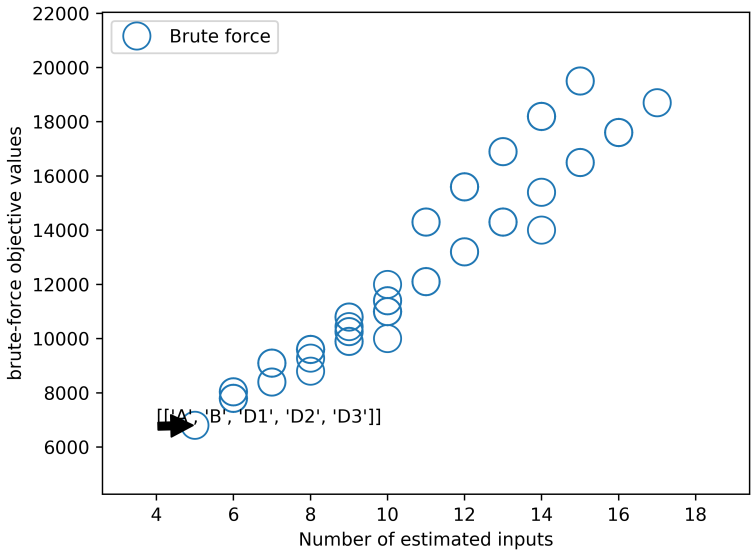

Figure 3.7: Brute force solutions with the best solution marked

3.4.3. Performance

The performance of the algorithms refers to the time taken to find solution. Continuing the use of variable complexity problem graphs, time is measured for the graphs generated with varying number of disciplines. A random target surrogate function is selected from the graph generated. Based on this target surrogate function, the time taken to find an optimum surrogate graph is calculated for the different algorithms. The resulting time chart is shown in figure 3.9 given below.

The topological method and the adjacency method, both can be scaled up to a high number of disciplines. However, the unreliability of the topological method seen in the verification section is also visible in the time distribution. For a particular number of disciplines, for example at 15, the time taken varies for the different graphs generated and for every target surrogate function. The distribution for the adjacency method is more uniform.

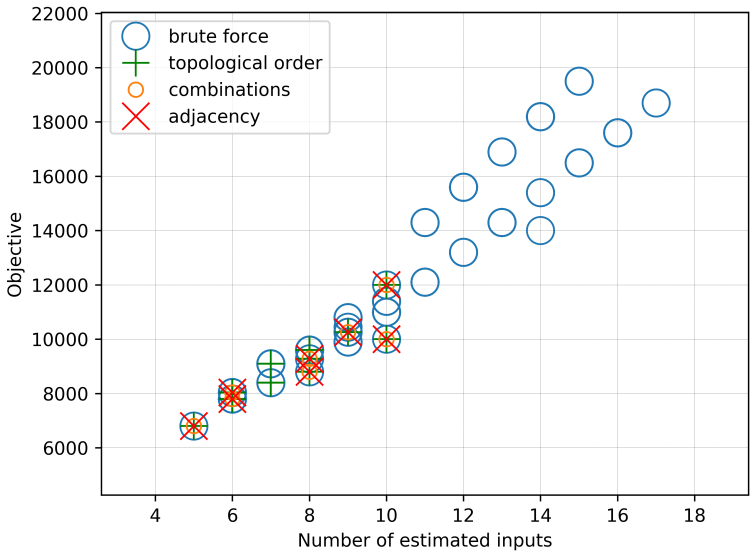

Figure 3.8: Solutions obtained from combinations, topological and adjacency methods compared with brute force solutions

Table 3.2: Verification of topological, combination and adjacency method against brute force method

Method	Successful evaluation	Error percentage	Unresolved percentage
Topological	92.4	1	6.6
Adjacency	99.3	0.7	0

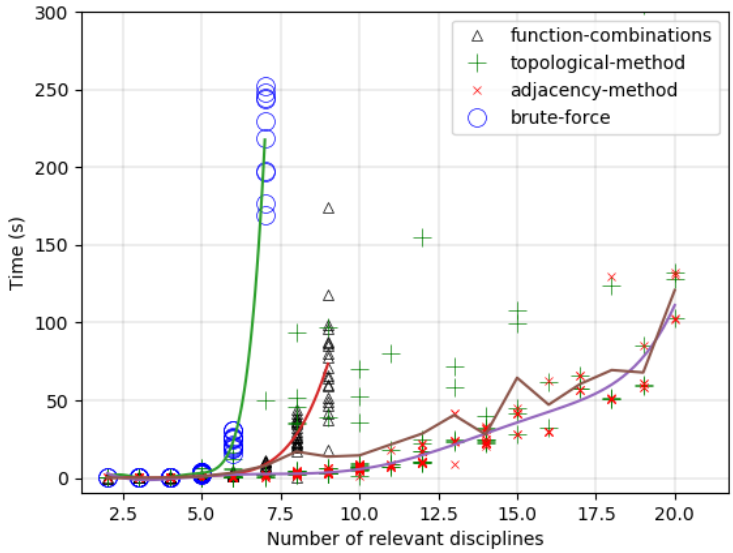

Figure 3.9: Time performance comparison for the 4 methods

4

MDO formulation

The purpose of the surrogate modeling method developed previously in this work has been to enable Multidisciplinary Optimization (MDO) with reduced computational effort. The problem that we want to study using MDO still needs to be defined. Various factors are taken into account when constructing an MDO problem. The MDO problem that is to be solved in an MDO exercise is of the form given below as shown in de Weck et al. [11]. It indicates the various factors within MDO.

$$s.t\ g(x,p) < 0,\ h(x,p) = 0$$

(4.1)

The objective is represented by the function f which has to be optimized based on the design variables x to find a minimum value. The variables p remain constant in the operations and represent values such as material density, fluid viscosity, etc. The values for the design variables are bound by the upper and lower limits specified through $x_{i,UB}$ and $x_{i,LB}$. The functions g and h represent inequality and equality constraints. The objective function f is a simplified representation of the analysis performed to calculate the objective value. In MDO, this objective value is obtained by evaluation through multiple disciplines. In order to present the MDO problem thus a description of the individual analysis tools as well their non-variable parameters (represented by p) is given in section 4.1.

4.1. Analysis Tools

An overview of the tools available from the repository is given previously in table 1.1. These are the in-house tools developed at TU Delft. The calculation methods employed in the analysis tools are useful in understanding the design that is arrived at. This is since the tools are modified for application in the current case.

Q3D: The Q3D tool (Quasi 3 dimensional), is based on the integration of 2-dimensional analysis tools, AVL, XFOIL, and VGK. Q3D is run in two modes - viscid and inviscid.In the inviscid mode, the tool makes use of AVL. AVL is based on the vortex lattice method and can provide accurate load distribution on the wing for the subsonic region. Additionally, compressibility corrections have been applied in AVL to extend the capability to flows with weak shocks.

In the viscous mode, the tools makes use of a combination of XFOIL and VGK tools. In the current analysis, the tool was further modified. The multidisciplinary optimization requires iteration to create a converged design due to the coupling between the different tools.Previously, Q3D made use of VGK to solve for compressible flows. However, VGK has difficulties in convergence at lift coefficients 0.58 and higher. Since the initial point obtained from literature was very close to this limit, Q3D was modified to function using XFOIL and avoid the limitation of VGK.

If we look at the drag coefficient breakdown as explained in Roskam [62], the different components are:

$$C_{D,wing} = C_{D_{0,wing}} + C_{D_{L,wing}} \tag{4.2}$$

$$C_{D_{0,wing}} = C_{D_{f,wing}} + C_{D,wave} \tag{4.3}$$

In Q3D while $C_{D_{L,wing}}$ (drag coefficient due to lift) and $C_{D_{f,wing}}$ (zero-lift drag coefficient) are computed using AVL and XFOIL, the wave drag ($C_{D,wave}$) is computed using VGK. As a result, the wave drag component from the total drag could not be computed by Q3D itself and hence a constant wave drag coefficient of 0.0022 to the total drag coefficient was added. The value of 0.0022 was chosen as a percentage of the overall drag. From aircraft similar to D-150 which fall under the category of commercial transport jet, the historical value of wave drag percentage was used. The additional effect of this simplification was that sweep was removed from the design variables. This was since sweep is a factor which affects wave drag.

EMWET : EMWET was developed with the specific purpose of application in MDO. Hence, the evaluation times for EMWET are low. It works via a two step process. In the first step, based on the aerodynamic loads, the wing box weight is estimated. Analytical methods are used for this purpose. In the second step using a correlation obtained from simulations for different aircrafts, the complete wing weight is obtained. The correlation between the wing box weight and the total wing weight is as follows:

$$W_W = 10.147 W_{calc}^{0.8162} \tag{4.4}$$

where W_W is the total wing weight and W_{calc} is the wing box weight. The material used within EMWET is aluminium 2024 alloy.

PROTEUS: PROTEUS functions as an aeroelastic tailoring tool. The application of composites for the advantages rendered by aeroelastic tailoring to achieve performance objectives was the primary driving force behind the development of PROTEUS. While the studies did previously were able to study specific responses in the wing due to the presence of composites. PROTEUS served as a preliminary design tool with the ability to perform static and dynamic aeroelastic analysis. The optimization routine combined with the analysis outputs minimizes the wing weight within the structural constraints set by strain and buckling.

Besides the primary aerodynamic loads due to air, non-structural masses (fuel and engine) are included in the calculation of loads on the wing. EMWET also considers the non-structural masses of fuel and engine weight and thus allows for a better comparison between the optimizations performed by the two tools.

Even though the PROTEUS tool successfully calculates the wing box weight, in its application to MDO an addition of secondary weight to the primary wing weight is required to calculate the complete wing weight. Hence, the correlation used between the wing box weight (primary wing weight) and the complete wing weight in EMWET, is extended for use in PROTEUS. So the relation 4.4 is used in calculating the complete wing weight using PROTEUS.

SMFA: The SMFA tool calculates the fuel for the mission based on the Brequet range equation. It makes use of the aerodynamic coefficients (C_L and C_D) at cruise conditions. Additionally, SMFA assumes the cruise condition fuel requirement as a fraction of the total fuel mass. This is to accommodate the other segments of the flight mission which include, take-off and landing, taxi, takeoff, climb, and descent.

$$\begin{aligned} exp &= RangeSFC/(speed\frac{C_{D,wing}+C_{D,WA}}{C_{L,wing}}) \\ fuel\ mass &= (1 - \frac{fuel\ fraction\ factor}{exp})MTOW \end{aligned} \tag{4.5}$$

Though the aerodynamic coefficients are obtained from Q3D and calculated for each design point, the wing-less aircraft drag ($C_{D,WA}$) is assumed constant. $C_{D,WA}$ was calculated from data available for an aircraft similar to D-150 which is the airbus A-320. The wing-less aircraft drag consists of the skin-friction drag and hence based on an estimate of the surface area. To calculate the wing-less aircraft drag, the following calculations are used.

$$\begin{aligned} A_t &= A_{wing} + A_r \\ D_{WA} &= C_f q \frac{A_r}{A_t} \\ C_{D,WA} &= 2\frac{D_{WA}}{\rho v^2 A_{wing}} \end{aligned} \tag{4.6}$$

The wetted area of the rest of the aircraft A_r is obtained based on the total wetted area A_t obtained from figure 40.17 in Obert [51] which presents the friction coefficients of various aircrafts along with the total wetted area. The drag coefficient $C_D WA$ obtained in this manner is used for the calculation of fuel as shown in eqn 4.6.

MTOW: The MTOW tool simply adds the weights obtained from the analysis and gives the maximum take-off weight (MTOM) and the zero fuel mass (ZFM). It consists of the folowing equations:

$$\begin{aligned} MTOM &= mWA + mFuel + mWingStructure \\ mZFM &= mWA + mWingStructure \end{aligned} \tag{4.7}$$

where mWA, mFuel and mWingStructure represent the wingless aircraft mass, fuel mass and the complete wing mass respectively.

4.2. MDO problem

In order to perform the design study, the D150 aircraft configuration is used as the base model which acts as an initial point.The D150 aircraft is representative of an Airbus A320 class aircraft.
The selection of the objective is such that the factor is affected by multiple design disciplines in an inverse manner leading to a situation where compromise has to be made between multiple tool output values. In the current case, to reduce fuel weight is pursued as an objective. The design variables used in the optimization are given in table 4.1 along with the upper and lower bounds.

Table 4.1: Design variables with their upper and lower bounds.

Design variable	Upper bound	Lower bound
Aspect ratio	13	8
Taper ratio 1 (λ_1)	0.8	0.5
Taper ratio 2 (λ_2)	0.4	0.2
Span(m)	37	30

Table 4.2: Constraints employed

Constraints
$V_f < V_{fueltank}$
$(W/S) \leq (W/S)_{ref}$

Table 4.3: Load case for the EMWET based optimization.

LC (Load case)	Mach No	EAS(m/s)	Load factor	H(m)
1	0.78	125	2.5	11000

Two constraints used in the design are also included (table 4.2. The first constraint limits the fuel volume to be less than the available volume within the wing. The wing loading constraint limits the amount of run-way length required. Thus, the aircraft can take-off and land from standard runways.

While the design variable and the constraints remain similar for the composite design case, the loadcases applied are different. This is due to the ability of PROTEUS to consider multiple loadcases in the design of a composite wing. The loadcases applied in the case of design using PROTEUS is given in the table 4.4 below.

Table 4.4: Load cases for the PROTEUS based optimization.

LC (Load case)	Mach No	EAS(m/s)	Load factor	H(m)
1	0.74	155	-1	7500
2	0.89	185	2.5	7500
3	0.89	143	1	11000

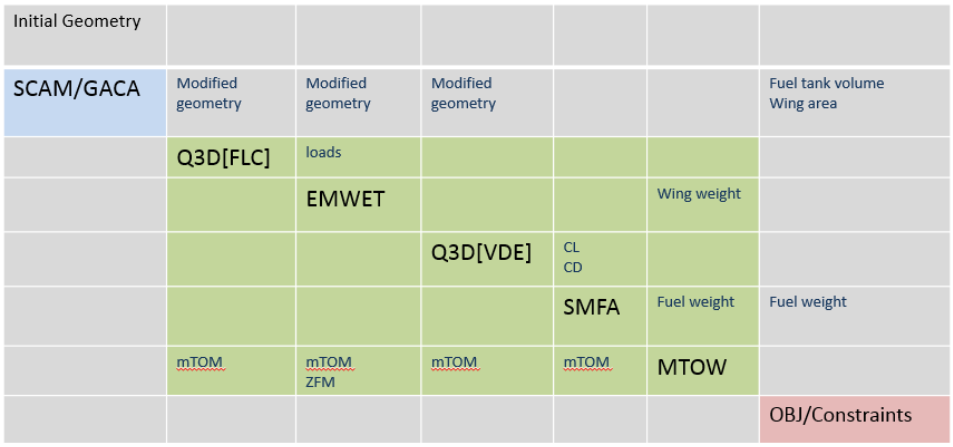

Figure 4.1: N2 chart for EMWET based MDO problem

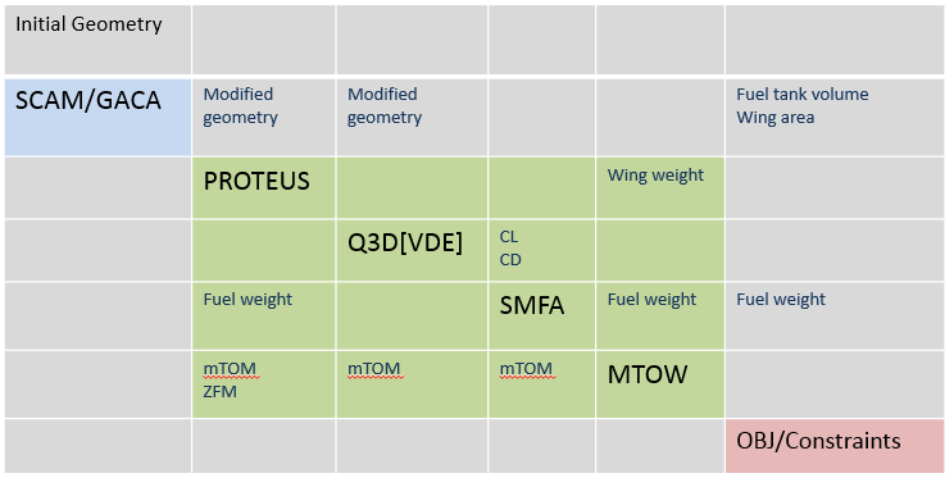

Figure 4.2: N2 chart for PROTEUS based MDO problem

An easier representation of the MDO problem for the two cases is provided in terms of the N2 chart. This representation is done in figures 4.1 and 4.2.

In order to complete the description of the MDO problem the reference values for the D-150 configuration are presented in table 4.5. The operating values of design range, mach cruise and cruise altitude remain constant throughout the optimization. Additionally, since D-150 is an open source configuration, it can be used in further studies based on the surrogate modeling methodology present in this report. It serves as the common baseline configuration.

4.3. MDO workflow

The previous sections develop the MDO problem in terms of the inputs and outputs of the various tools to minimize the objective which is fuel. In order to execute this MDO problem, the automation capability provided by KADMOS is used to create the executable workflow files. The outputs obtained can be visualized as XDSM graphs. The MDO problem is formed into a fundamental problem graph (FPG). With the knowledge of FPG, suitable computational architecture can be added to obtain the MDAO

graph. The process is presented in section 3.1 and can be revisited for reference.

4.3.1. EMWET based

The EMWET based workflow is representative of the metallic wing optimization. In order to perform the optimization, an optimization framework has to be superimposed upon this problem. For the current work, the analysis is limited to the use of a single framework which is the $MDF-GS$. With this framework superimposed upon the FPG, the resulting executable workflow can be seen in the figure given below.

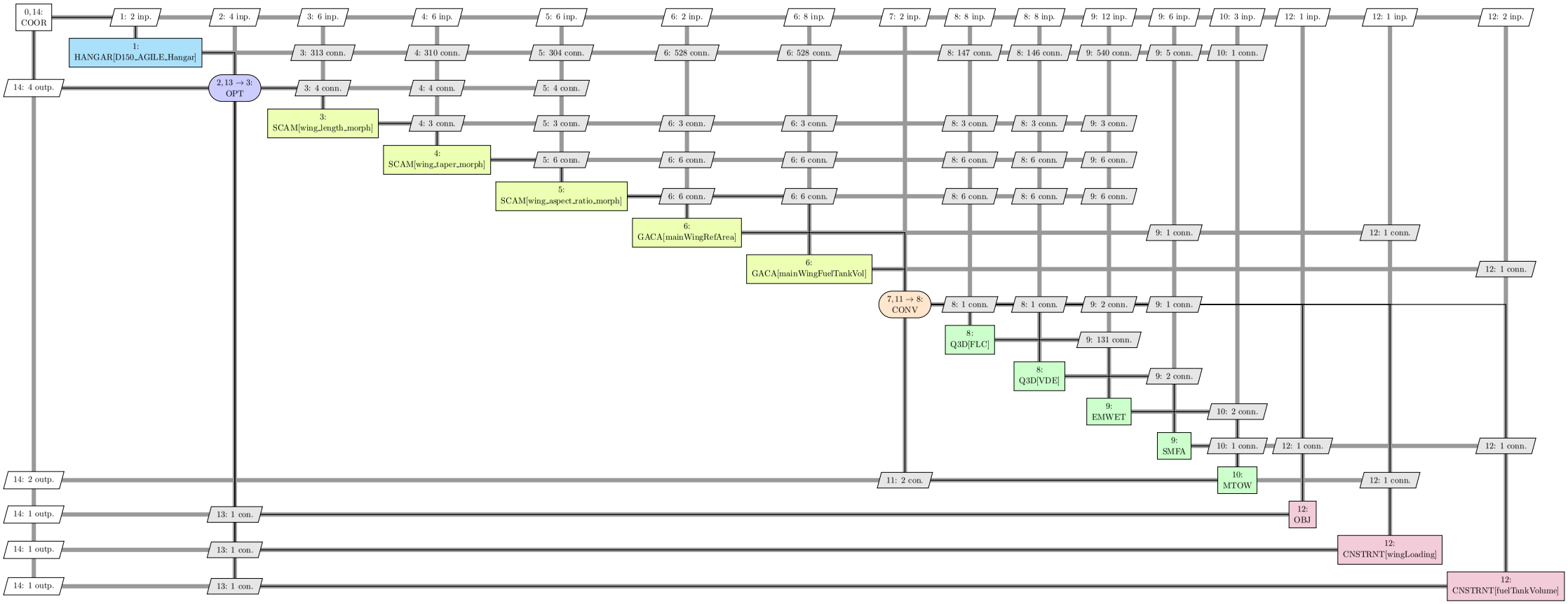
0, 14: COOR
1: 2 inp.
2: 4 inp.
3: 6 inp.
4: 6 inp.
5: 6 inp.
6: 2 inp.
6: 8 inp.
7: 2 inp.
8: 8 inp.
8: 8 inp.
9: 12 inp.
9: 6 inp.
10: 3 inp.
12: 1 inp.
12: 1 inp.
12: 2 inp.
1: HANGAR[D150_AGILE_Hangar]
3: 313 conn.
4: 310 conn.
5: 304 conn.
6: 528 conn.
6: 528 conn.
8: 147 conn.
8: 146 conn.
9: 540 conn.
9: 5 conn.
10: 1 conn.
14: 4 outp.
2, 13 → 3: OPT
3: 4 conn.
4: 4 conn.
5: 4 conn.
3: SCAM[wing_length_morph]
4: 3 conn.
5: 3 conn.
6: 3 conn.
6: 3 conn.
8: 3 conn.
8: 3 conn.
9: 3 conn.
4: SCAM[wing_taper_morph]
5: 6 conn.
6: 6 conn.
6: 6 conn.
8: 6 conn.
8: 6 conn.
9: 6 conn.
5: SCAM[wing_aspect_ratio_morph]
6: 6 conn.
6: 6 conn.
8: 6 conn.
8: 6 conn.
9: 6 conn.
6: GACA[mainWingRefArea]
9: 1 conn.
12: 1 conn.
6: GACA[mainWingFuelTankVol]
12: 1 conn.
7, 11 → 8: CONV
8: 1 conn.
8: 1 conn.
9: 2 conn.
9: 1 conn.
8: Q3D[FLC]
9: 131 conn.
8: Q3D[VDE]
9: 2 conn.
9: EMWET
10: 2 conn.
9: SMFA
10: 1 conn.
12: 1 conn.
12: 1 conn.
14: 2 outp.
11: 2 con.
10: MTOW
12: 1 conn.
14: 1 outp.
13: 1 con.
12: OBJ
14: 1 outp.
13: 1 con.
12: CNSTRNT[wingLoading]
14: 1 outp.
13: 1 con.
12: CNSTRNT[fuelTankVolume]

Table 4.5: D150 reference values from Gu et al. [27]

Parameter	Value	Unit
Design range	4000	km
Mach cruise	0.78	-
Wing span	33.74	m
Reference area (S_{ref})	463.2	m^2
Cruise altitude	10668	m

4.3.2. PROTEUS surrogate based

In order to construct the PROTEUS surrogate based framework, intermediate workflows were implemented which have been presented in this section along with the resulting final workflow. A flowchart showing the steps to perform the composite optimization using PROTEUS is shown in figure 4.3. An additional step is added in order to include the deformation of the wing in flight mode. This addition to the geometry allows a more accurate estimate of the aerodynamic coefficients using Q3D.

Building PROTEUS surrogate

As presented earlier surrogate modeling is an estimation problem and hence data needs to be generated which can be used to create a model representative of the tool. The development of the optimum surrogate graph strategy supports the development of the surrogate due to the run time for PROTEUS. In the current study, the time taken is higher than 24 hours for single PROTEUS simulation. Using the surrogate modeling methodology, the design of experiments (DOE) workflow created is shown in figure 4.4.

The workflow thus developed is used to generate PROTEUS data based on Latin-hypercube sampling McKay [48]. The purpose of using Latin-hypercube sampling is to get an even distribution over the design space. An overview of Latin-hypercube sampling is provided in Queipo et al. [59]. Since, there are 4 design variables along with 2 variables from the couplings, 60 (10 design points for every additional input variable) samples obtained. The variable range for the data sampling is the same as the range for the MDO problem in the case of the design variables. For the other two variables, a range is estimated based engineering estimate for aircraft of the A-320 class. The design range for these two variables is provided in table 4.6.

Variable	upper bound	lower bound
Fuel weight	15000	7000
Max take-off weight	70000	55000

Table 4.6: Upper and lower limits for the additional input variables in the creation of PROTEUS surrogate

The consequent surrogate model developed is evaluated for its accuracy. For this purpose, the k-fold validation method is implemented. The advantage of using k-fold validation is to reduce bias in the model. The accuracy is measured for multiple subsets of data obtained from the overall set. Thus, all the data can be used for training and testing purposes. The error for the various cases is calculated using the root mean square error (RMSE) 4.8.

$$RMSE = \sqrt{\frac{\sum_{i=1}^{N} (Predcited_i - Actual_i)^2}{N}} \tag{4.8}$$

The root mean square error in wing weight is given in figure 4.5 for the possible cases in a k-fold validation.

Wing aeroelastic deformation

For the steady state flight, the aircraft wing deflections due to aircraft loads can be obtained from PROTEUS which was not possible for EMWET. In order to obtain the deflections, the laminate distribution obtained for the optimized design points is used. The resulting deflected shape is analyzed using Q3D viscous mode in order to create a surrogate version for the aerodynamics analysis.

The aeroelastic analysis with the deformed shape can be explained in two steps with the figurative representation in figure 4.6.

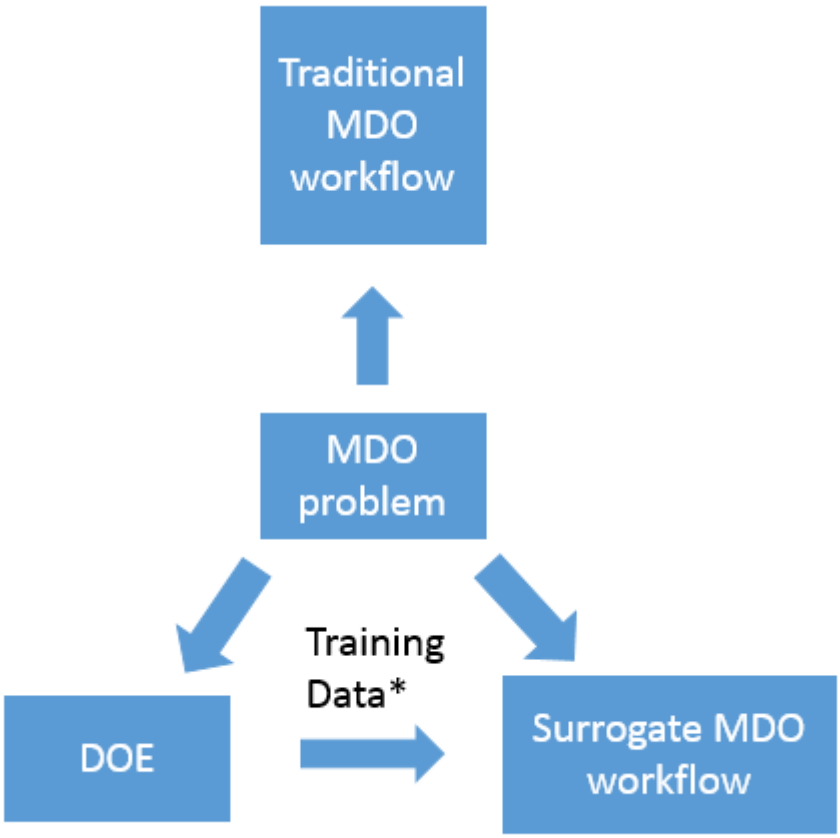

Figure 4.3: Overview of the relation between surrogate modeling and surrogate based MDO. (* - represents the modification done to the training data to include 1-g deformation in cruise condition)

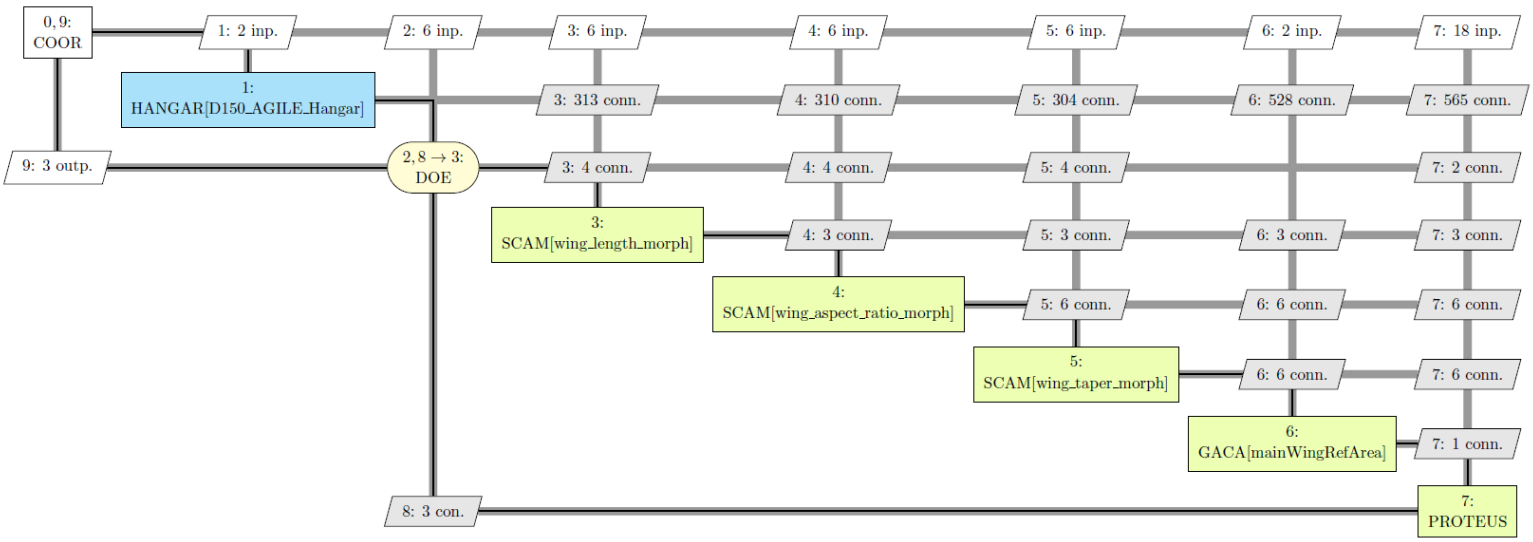

Figure 4.4: The workflow for generating the PROTEUS surrogate data

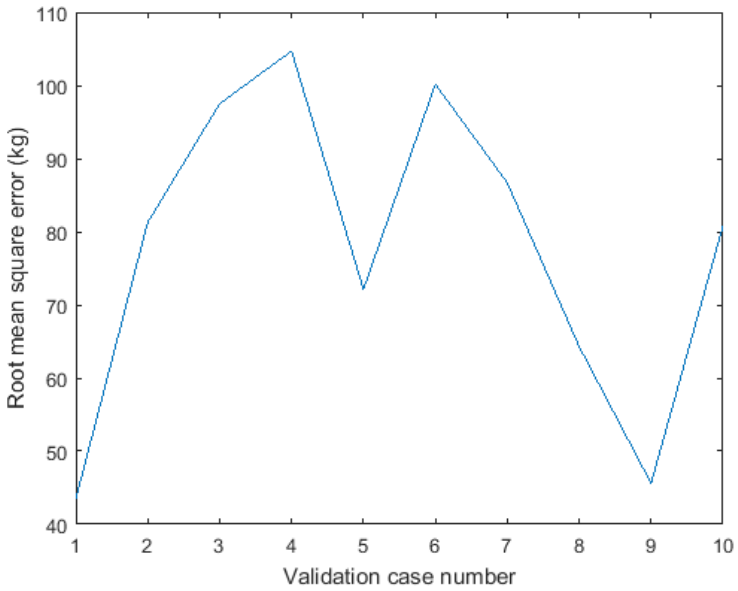

Figure 4.5: Error values for k-fold validation cases

1. In the first step, the optimized laminate distribution is obtained. This represents the previous section where the design of experiments is performed over the design space. Along with the wing weight, the corresponding optimized laminate distributions are obtained as well.
2. In the second step, the optimized laminate distribution is used as an input to PROTEUS. As a result when the steady state cruise loads are applied the deflections are calculated using the optimized laminates. These deflected shapes are used as input to Q3D viscous analysis which calculates the aerodynamic coefficients for the modified shape.

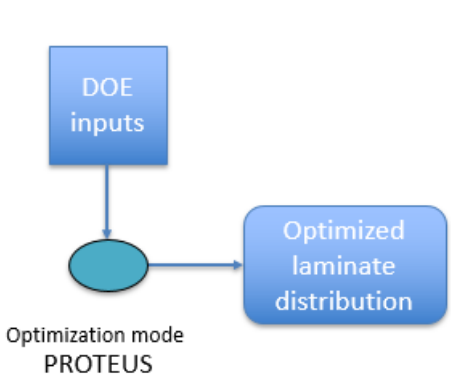

(a) Creation of the surrogate data

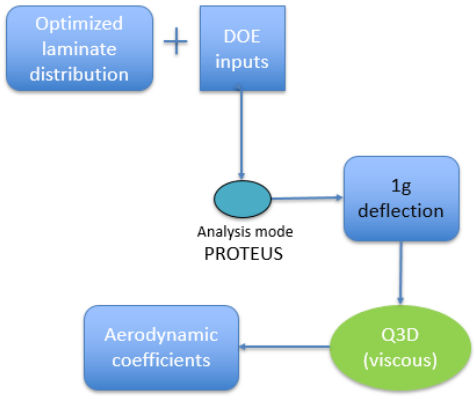

(b) Processing the optimized data to obtain the aerodynamic coefficients for deflected shapes

Figure 4.6: Steps to obtain deformed wing shape aerodynamic coefficients

With the resulting aerodynamic coefficients data, a surrogate model for the aerodynamic analysis is used in place of the Q3D analysis. This interpolates the aeroelastic analysis over the design space and thus approximates the passing of the deflected shape from PROTEUS to Q3D. For the surrogate model created the accuracy of the models is estimated using the k-fold validation method. The percentage error for the various cases of validation is given in figure 4.7.

The average error for the Q3D surrogate model and the PROTEUS model is summarized in table 4.7.

Building PROTEUS based MDO

The objective of creating the PROTEUS surrogate was for implementation in the MDO workflow. Upon replacing the PROTEUS and Q3D functions with the surrogate function we obtain the MDO workflow on the next page.

This represents the executable form of the original MDO problem which was discussed in section 4.2. The final executable file in the form of the CMDOWS format is based on this workflow and run via the openMDAO platform.

Thus, the construction of the two workflows necessary for the study is presented until now. With the construction of the PROTEUS based MDO workflow and the EMWET based workflow, the focus can then be shifted towards the validation of the surrogate based workflow for PROTEUS and the optimization outputs generated.

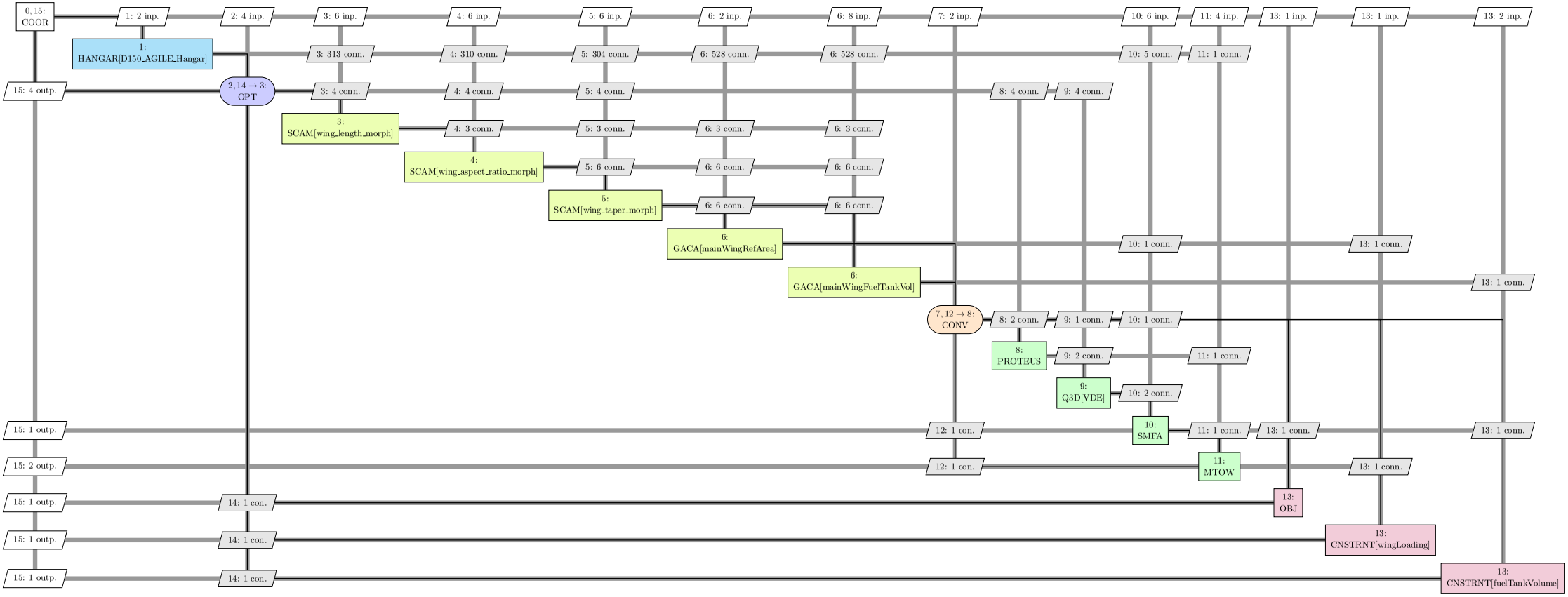
0, 15: COOR
1: 2 inp.
2: 4 inp.
3: 6 inp.
4: 6 inp.
5: 6 inp.
6: 2 inp.
6: 8 inp.
7: 2 inp.
10: 6 inp.
11: 4 inp.
13: 1 inp.
13: 1 inp.
13: 2 inp.
1: HANGAR[D150_AGILE_Hangar]
3: 313 conn.
4: 310 conn.
5: 304 conn.
6: 528 conn.
6: 528 conn.
10: 5 conn.
11: 1 conn.
15: 4 outp.
2, 14 → 3: OPT
3: 4 conn.
4: 4 conn.
5: 4 conn.
8: 4 conn.
9: 4 conn.
3: SCAM[wing_length_morph]
4: 3 conn.
5: 3 conn.
6: 3 conn.
6: 3 conn.
4: SCAM[wing_aspect_ratio_morph]
5: 6 conn.
6: 6 conn.
6: 6 conn.
5: SCAM[wing_taper_morph]
6: 6 conn.
6: 6 conn.
6: GACA[mainWingRefArea]
10: 1 conn.
13: 1 conn.
6: GACA[mainWingFuelTankVol]
13: 1 conn.
7, 12 → 8: CONV
8: 2 conn.
9: 1 conn.
10: 1 conn.
8: PROTEUS
9: 2 conn.
11: 1 conn.
9: Q3D[VDE]
10: 2 conn.
15: 1 outp.
12: 1 con.
10: SMFA
11: 1 conn.
13: 1 conn.
13: 1 conn.
15: 2 outp.
12: 1 con.
11: MTOW
13: 1 conn.
15: 1 outp.
14: 1 con.
13: OBJ
15: 1 outp.
14: 1 con.
13: CNSTRNT[wingLoading]
15: 1 outp.
14: 1 con.
13: CNSTRNT[fuelTankVolume]

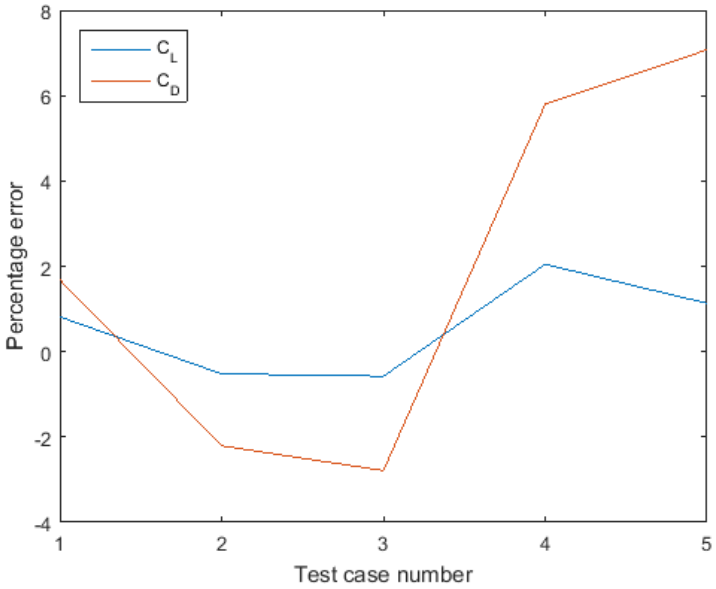

Figure 4.7: Percentage error

Analytical tool	Interpolation model	Average Error	
$PROTEUS$	Kriging	Root mean square 77.68 kgs	
$Q3D^*$	Kriging		Percentage error
		C_L	1.01
		C_D	3.91

Table 4.7: Average errors for the surrogate models created

4.4. MDO workflow validation

The workflow created for the MDO problem needs to be tested for the accuracy of the analysis performed by the design tools. This verification helps to make sure the modeling parameters of the tools are correct along with the exchange of values between the various tools. The aircraft case for which the MDO problem is formulated is the D-150 and thus the same configuration is used for the multidisciplinary analysis (MDA).

The resulting analysis values are presented in table 4.8. In the table the values are compared with a similar analysis performed by Gu et al. [28].

Mass(kg)	Conceptual	VLM (%)	Euler-CFD(%)	Q3D-EMWET (%)
MTOM	76168	-2.5	5.9	-1.4
MFM	13142	-12.9	29.1	20.2

Table 4.8: Multidisciplinary analysis of the Q3D-EMWET based system compared to previous data.

The higher fuel consumption in the case of Euler-CFD analysis is due to the overestimated wave drag as has been explained by the author in Gu et al. [28]. For the case of Q3D-EMWET, since the wave drag estimation is modeled, the value of the constant magnitude wave drag was thus set to a value to emulate the Lift/drag ratio of a commercial jet. A reference for the various Lift/drag is provided in the text by Obert [51]. A constant value is thus set for the wave drag coefficient. The resulting aerodynamic parameters for the initial design point are presented in table 4.9 along with the reference data from the literature. One cause of the difference between the values is due to the difference in the ways the D-150 geometry is used. In the case of the reference, an initial geometry is generated using VAMP zero . This thus creates a wing design with differences in geometry parameters to the one used in the current study. The higher lift coefficient results in a higher lift induced drag and thus a higher

overall drag. This is also the cause for the comparatively higher maximum fuel mass for Q3D-EMWET in table 4.8.

	Conceptual	VLM	Euler-CFD	Q3D-EMWET
C_L	0.584	0.562	0.622	0.629
C_D	0.0304	0.0271	0.0451	0.0334

Table 4.9: Aerodynamic coefficients of the Q3D-EMWET based system compared to previous data.

The additional parameter of comparison for the case in the wing weight estimation which compared to the wing weight for an aircraft similar to the D-150. In this case, the Airbus A320-200 data is used from Obert [51].

The wing weight for the airbus aircraft is given as 8801 kg while the weight obtained using EMWET in the current analysis is 9311 kg. The difference in weight is 5.7 % and thus gives confidence in the modeling parameters for the EMWET tool used for metallic weight estimation.

The comparison of the values obtained for the various tools used in the analysis thus indicates that the modeling parameters are thus sufficient to analyze the various design points which would be obtained while the optimizer searcher for an optimum design.

5

Results and Discussion

While the results in the previous sections presented the development of the framework, the focus now is towards the insights made available by the application of this framework. The optimizations performed using the EMWET based workflow and the PROTEUS based workflow lead to the metal based planform and composite based planform respectively. In order to make these optimizations possible, PROTEUS surrogate was used instead of the physics based version of PROTEUS. Additionally, the cruise deformation of the wing was included. The results for these two designs are further superimposed with a composite design using PROTEUS. Thus, three sets of results are formed.

1. Intermediate planform optimization
2. Final composite design.
3. Performance of final wing designs

For brevity, further on in the report, the final composite designs obtained via the two workflows are referenced as D1 and D2. D1 will be used for the composite design which is obtained after superimposing the composite design on intermediate planform obtained by the metal based workflow. Similarly, D2 will be used for the composite design obtained after superimposing the composite design on the intermediate planform obtained by the PROTEUS surrogate based workflow.

5.1. Tool sensitivity

The normalized tool outputs are generated for sensitivity plots. By varying a single input design variable from the lower bound to the upper bound the corresponding outputs were obtained. These bounds are used as defined in the MDO problem. Hence, two sets of sensitivity plots are obtained, one for each optimization and shown in figure 5.1a and figure 5.1b.

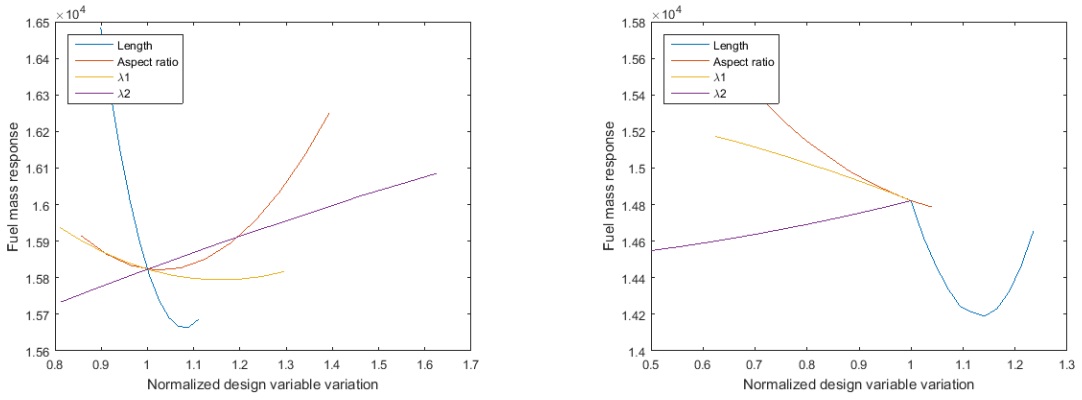

(a) Metal based design sensitivities

(b) Composite based design sensitivities

Figure 5.1: Plots of sensitivity for the composite and metal based design

The main indication to read from the graphs is the magnitude of change which occurs for the design variables. The increase or decrease in the design variable indicates the direction in which the optimizer is expected to move to find the optimum. Thus, in the wing optimization results, these changes are referred to check if the optimum is correct.The physical explanation for the sensitivity graph can be looked at for each design variable.

In the case of length, an increase indicates a more slender wing (higher aspect ratio) which causes the induced drag to reduce. However, after a certain point, the increase in wing weight negates the reduction in drag due to a higher aspect ratio.

The aspect ratio, based on the relation with induced drag, indicates a reduction in overall fuel mass due to an increase in aspect ratio.

5.2. Wing optimization

The optimizations performed using the EMWET and PROTEUS based workflows are discussed in this section. The differences caused in the planform design can be attributed to a difference in sensitivities. The tool sensitivities have hence been presented in the previous section which gives an understanding of how the initial design changes to achieve the optimum. The optimum planforms obtained using EMWET and PROTEUS surrogate have been shown in figure 5.2 along with the baseline design for comparison.

The primary difference between the two designs is present in terms of the aspect ratio. The composite wing is able to achieve a higher aspect ratio which can be attributed to the higher strength to weight ratio of the composite wing. It is hence able to carry the aerodynamic loads with a wing weight increase which does not negate the drag reduction benefits.

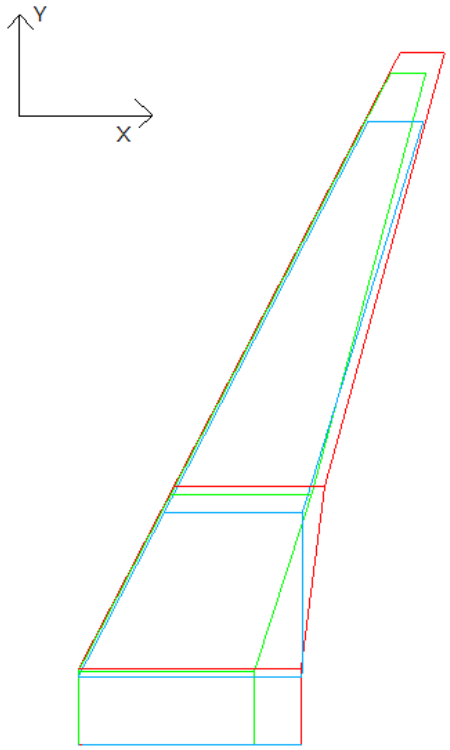

Figure 5.2: Baseline(Blue), metal(red) and composite (green) optimized wings.

For the individual design variables, the increase or decrease in the value of a particular variable is shown in table 5.1 and table 5.2 for the metal and composite designs respectively. The change is in agreement with the sensitivities in figure 5.1.

The convergence of the optimized design shown for the two cases in figures 5.3 and 5.4 displaying the objective, constraints and design variables. The optimized design is affected by the design bound-

Table 5.1: Initial and optimized design variables for metal design

Design variable	Initial	Optimized	Change
Length	16.95	21	↑
Aspect ratio	9.39	10.2	↑
λ_1	0.617	0.67	↑
λ_2	0.246	0.20	↓

Table 5.2: Initial and optimized design variables for composite design

Design variable	Initial	Optimized	Change
Length	17	20.38	↑
Aspect ratio	12.5	11.5	↓
λ_1	0.85	0.79	↓
λ_2	0.45	0.20	↓

aries in case of metal design with the length reaching the maximum value. The constraints remain inactive in the case of metallic design optimization.

In the case of the composite design while the design length value remained within the allowable design range the design was affected by the constraint value on the wing loading which was unsatisfied in case of the initial design. As a result, the optimizer moved towards a lower aspect ratio and thus satisfying the wing loading constraint. A further increase in length creates a higher aspect ratio. As a result, the length of the composite wing is shorter than the metallic wing.

The length and aspect ratio parameters display similar tendencies with a positive increase associated with a decrease in fuel weight. The composite wing, however, does have a noticeable higher aspect ratio which can be attributed to the use of composites. The magnitude of length is lower in composite wing compared to the metal wing,since a further increase would lead to an increase in wing weight and hence an increase in fuel consumption. While the taper ratio in the case of the metallic wing has a predictable sensitivity, the sensitivity in the case of the composite wing is dependent on the initial design. The taper sensitivity in the case of composite design is different based on the design point around which it is calculated. In order to choose the best design, hence, the one with the best fuel efficiency is chosen with a different initial design point set for each case.

5.3. Wing composite superimposition output

Once the planform designs for the metal based workflow and the composite based workflow are obtained, the final step in the methodology involves the superimposing the composite design upon the wing. This effectively means, the planform shape obtained is designed as a composite wing using PROTEUS. Since PROTEUS performs an optimization, the final design supersedes the previous design similar to a sequential optimization process.The resulting structural design is presented in terms of 4 properties by PROTEUS.

1. Buckling index
2. Strain index
3. Stiffness distribution
4. Laminate thickness

Strain and buckling index values represent normalized values with respect to the maximum allowable strain and buckling. Thus, the wing region with an index value of 1 represents strain and buckling critical regions. The structural properties of thickness and stiffness determine the wing design since they are used as inputs in order to determine the stacking of the laminates.

Metal superimposed composite

The metal superimposed composite designs will be referred to as D1 further on in the report. As described previously, the design output produced from PROTEUS is shown based on the 4 structural properties. The different loadcases create the loading conditions needed to evaluate the stresses.

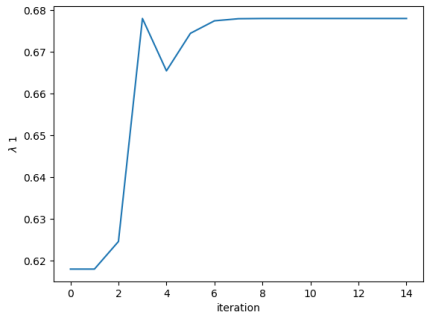

(a) Taper 1

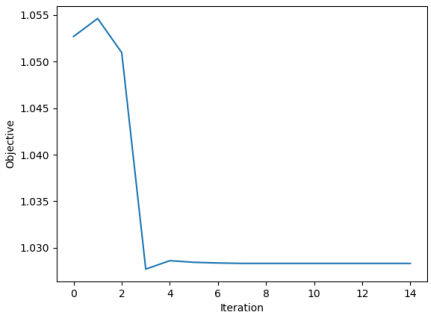

(b) Objective

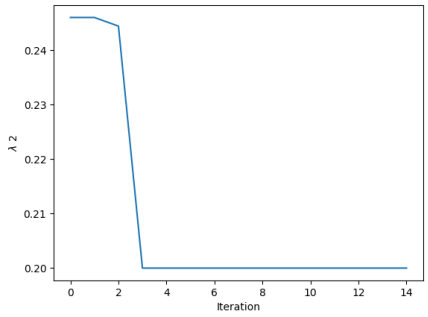

(c) Taper 2

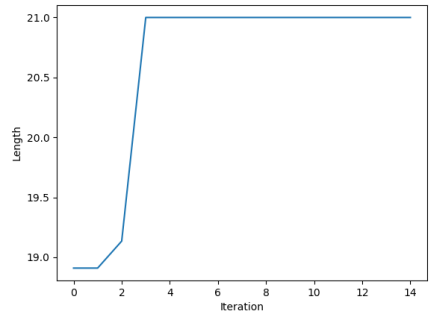

(d) Length

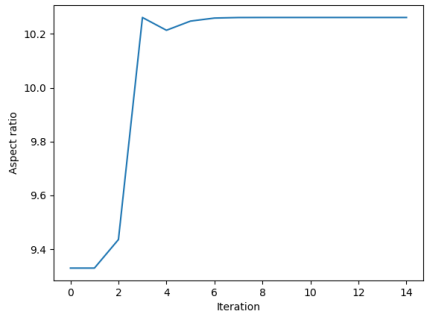

(e) Aspect ratio

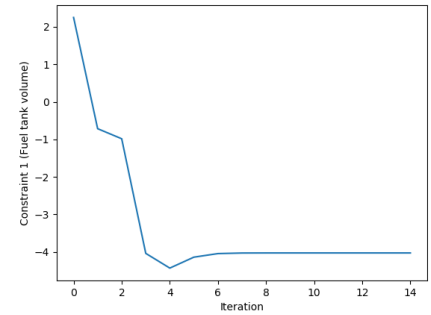

(f) Constraint 1

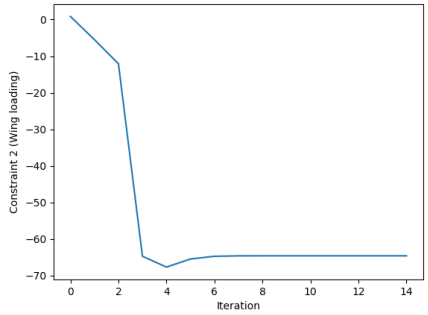

(g) Constraint 2

Figure 5.3: Optimization convergence for design variables of metal based design

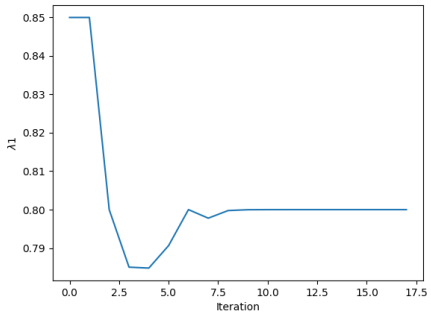

(a) Taper 1

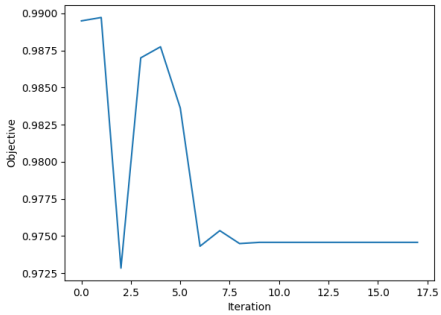

(b) Objective

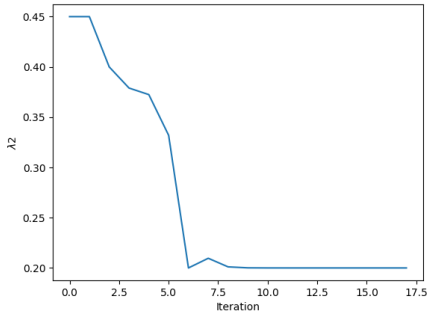

(c) Taper 2

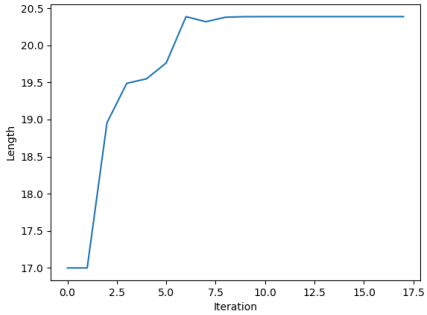

(d) Length

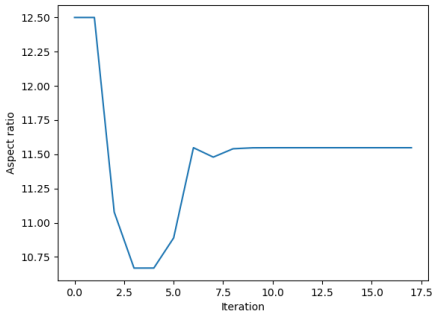

(e) Aspect ratio

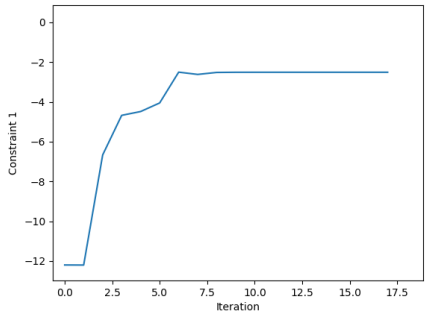

(f) Constraint 1 (fuel volume <tank volume

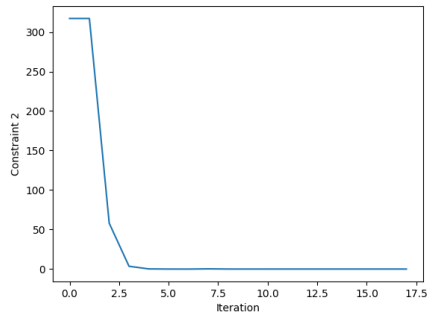

(g) Constraint 2 (Wing loading limit)

Figure 5.4: optimization convergence history for composite wing design

Several observations can be made for the design D1.

1. The buckling indices are presented in figures 5.5 which indicate that the indices are higher on the top-skin. The resulting aeroelastic tailoring can be observed for the out of plane stiffness distribution of the top skin in figure 5.8. Due to a comparatively lower buckling critical region, the lower-skin indicates a lack of in/out of plane stiffness distribution.

   While it can be argued that the thickness could be reduced for the lower-skin in order to create aeroelastic tailoring and thus reduce weight, the in-plane stiffness does not allow to do so. The lower skin is dominated by strain critical regions created due to load condition 2. Since the in-plane and out-of plane stiffness are not independent of each other the wing is tailored for the dominant strain critical regions through in-plane stiffness.

2. The strain failure index is active for both the top and lower skin. The strain critical regions if compared to the buckling critical regions show a larger region of impact. As a result, the aeroelastic tailoring in figure 5.8 shows in-plane stiffness which is oriented along the wing.

3. While the in-plane stiffness does align itself to cater to the strain critical regions, an additional effect is also created. The in-plane stiffness is oriented in the forward direction. Such a stiffness distribution creates a response resulting in wash-out at the wing tips. The reason for the optimizer to do this is to shift the aerodynamic center towards the wing root and thus reduce the bending moment in the outer regions. The reduced bending moment allows for a lighter wing.

4. The thickness of the wing presents an additional effect that the aeroelastic tailoring produces. The thickness of the wing shown in figure 5.8 is higher in the front part of the wing as compared to the rear. Such a shift in thickness is present in the top and lower skin with a more pronounced effect in the lower-skin. The front spar also has a higher thickness as compared to the rear spar. This forward shift in thickness moves the elastic axis of the wing forward and thus creates an additional wash out effect moving the aerodynamic center towards the wing root and reducing wing load at the wing tip.

5. While the thickness in the forward spar is higher than the rear spar in the rest of the wing, at the root we see a reverse trend. This is explained by the strain failure index comparison of the front and rear spar at the root. The strain failure constraint is active in the rear spar. Thus, in order to achieve the required strength, the optimizer increased the thickness at the root for the rear spar.

Composite design

The composite design is obtained from the superimposition of composite structure on PROTEUS based planform design. Further on in the report, this design is referred to as D2. The design observations which were presented for design D1 are also presented for the design D2 further below.

1. In terms of similarities, the critical regions for the different loadcases remain similar in design D1 and D2. The LC2 creates strain critical region on the top and bottom skin in the D1 and D2 designs alike with as can be seen in figures 5.6 and 5.12. In terms of buckling the failure index also present a similar effect fro the top-skin and lower skin for the two designs for the loadcases LC1, LC2 and LC3 based on the figures 5.5 and 5.9 for D1 and D2 respectively.

2. The stiffness distribution in the composite design D2 is dominated by in-plane stiffness which is shown in figure 5.13a. Since the in-plane and out-plane stiffness cannot be modified independently of each other the aeroelastic tailoring for out-plane stiffness is limited. The influential factor for the in-plane stiffness is observed from the strain failure index for LC2 in figure 5.11b. It shows that the top and lower skin are both dominated by critical index values which are not presented in the loadcases LC1 and LC3. Thus, LC2 can be considered as the major design driving constraint.

3. The thickness distribution in the design D2 creates similar load alleviation conditions as the design D1 with the shifting of the wing thickness towards the front as compared to rear in the top and rear skin.

The observation of the results presents that the two designs D1 and D2 have certain differences and certain similarities. While there is a difference in the magnitude of the parameters, the patterns for stiffness distribution and thickness can be considered to be similar.

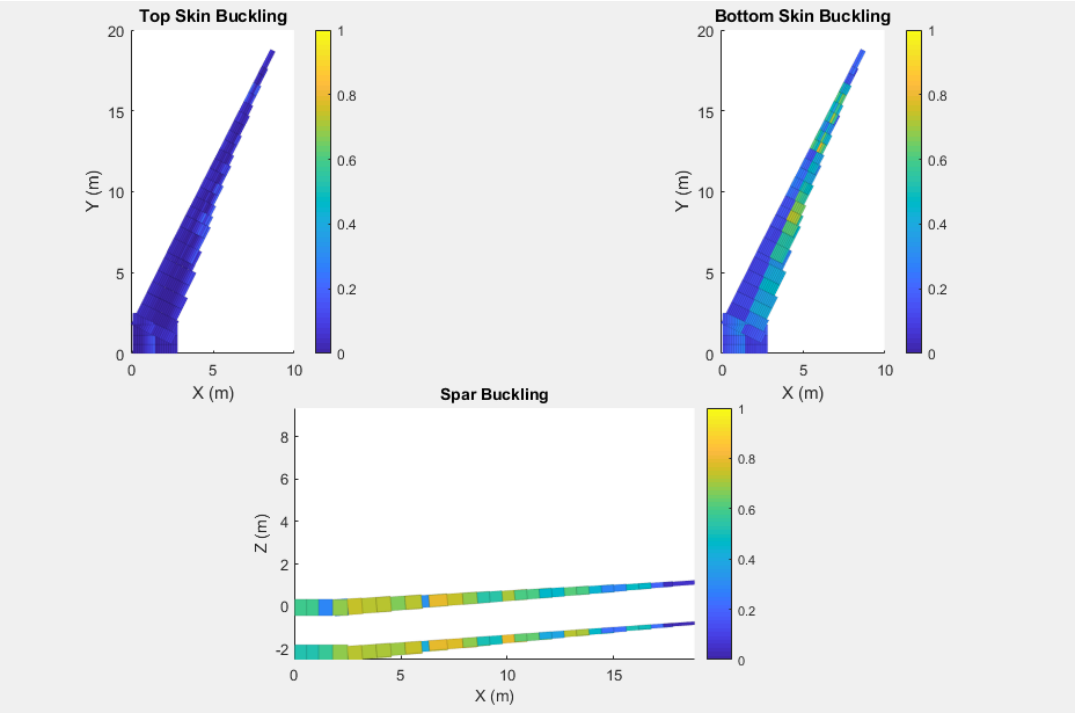

(a) Buckling index - locadcase 1

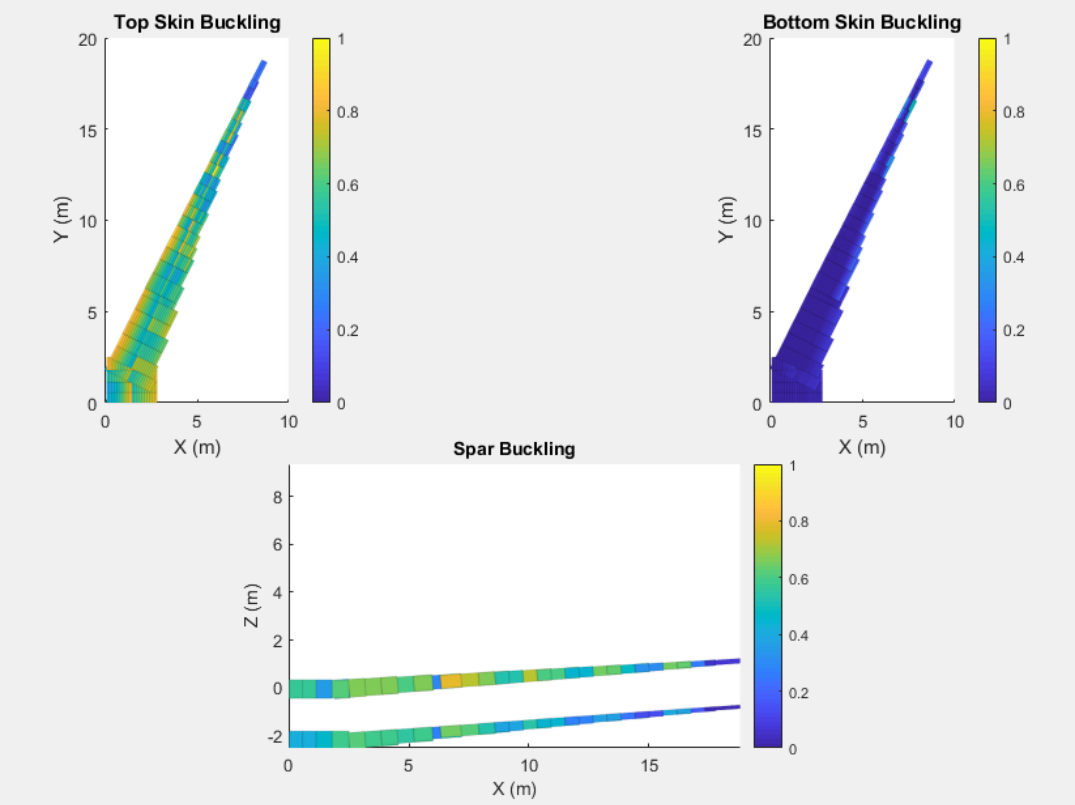

(b) Buckling index - locadcase 2

Figure 5.5: Buckling index for the different loadcases used in PRTOEUS for design D1.

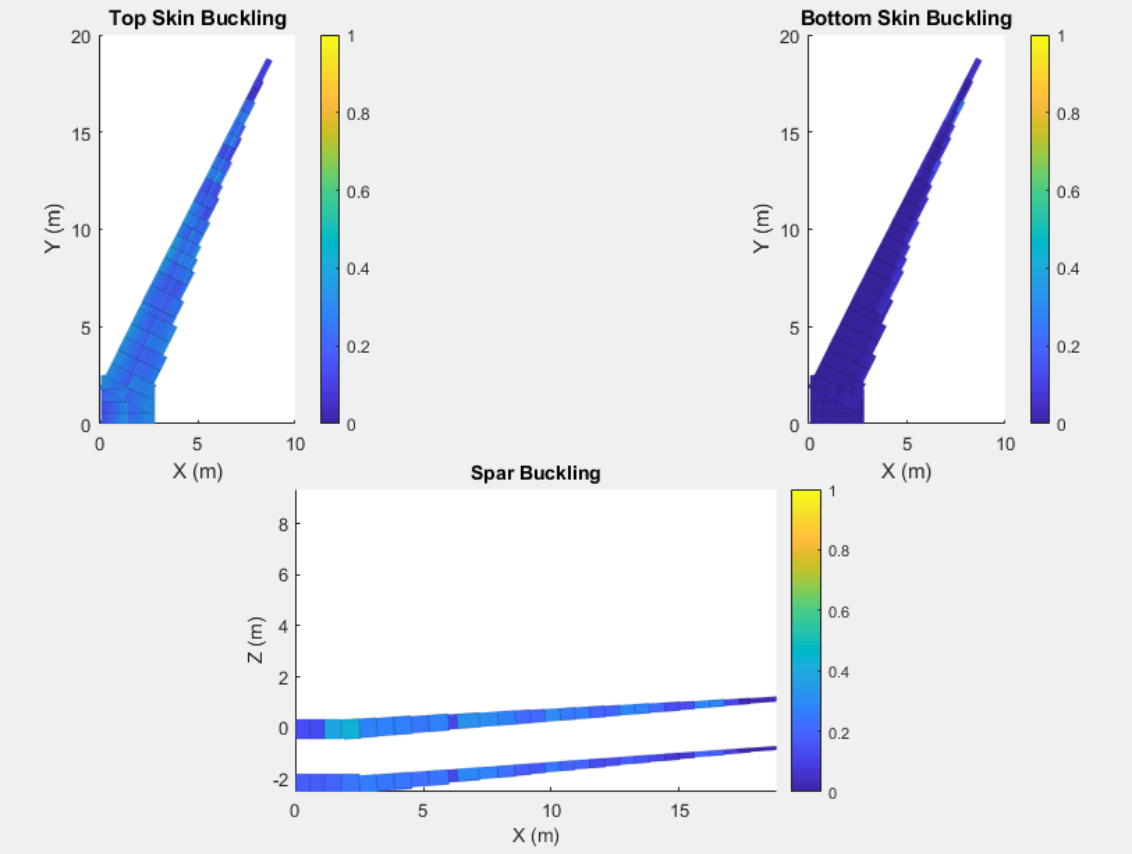

(c) Buckling index - locadcase 3

Figure 5.5: Buckling index for the different loadcases used in PRTOEUS for design D1. (**contd)

5.4. Performance comparison

The difference in performance for the two designs dictates the fuel efficiency. Reduction in fuel weight has the immediate effect of lower operational cost and also emissions in the long run. With the composite design obtained for the two methodologies based on EMWET based workflow and PROTEUS based workflow, the performance is estimated for the two design in terms of fuel weight. The results obtained in table 5.3 indicate a greater fuel efficiency for the PROTEUS based design D2.

Table 5.3: Fuel efficiency performance comparison for the designs D1 and D2 based on the two design methodologies

Parameter	Initial	Metal superimposed (D1)	Composite superimposed (D2)
Fuel	15803	14646	14371
Percentage reduction	-	7.3%	9.06%

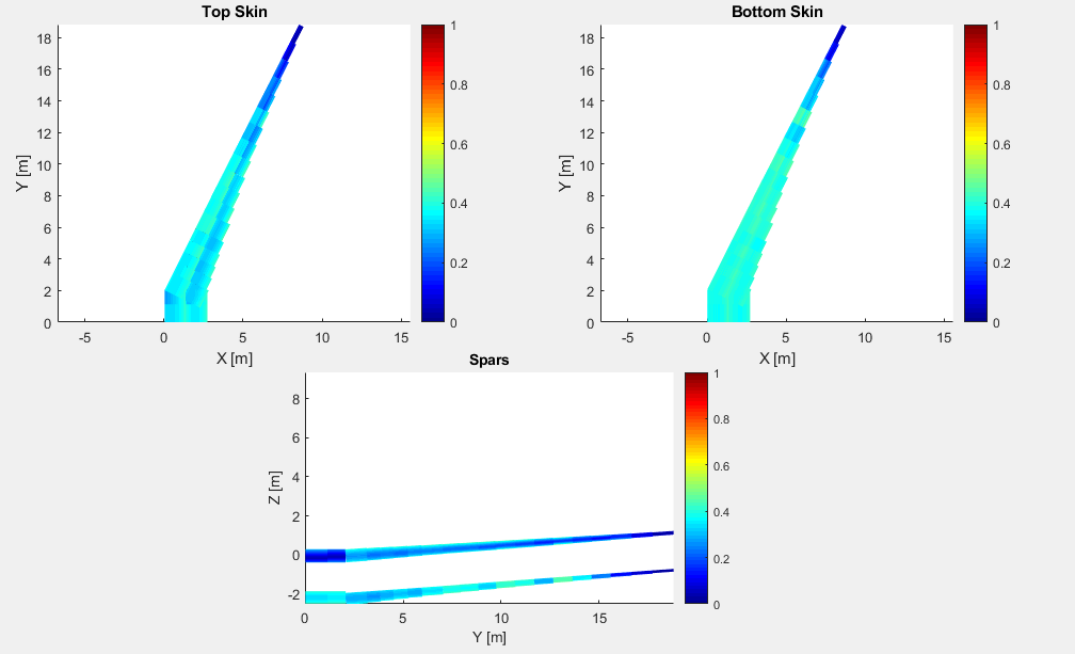

(a) Strain index -loadcase 1

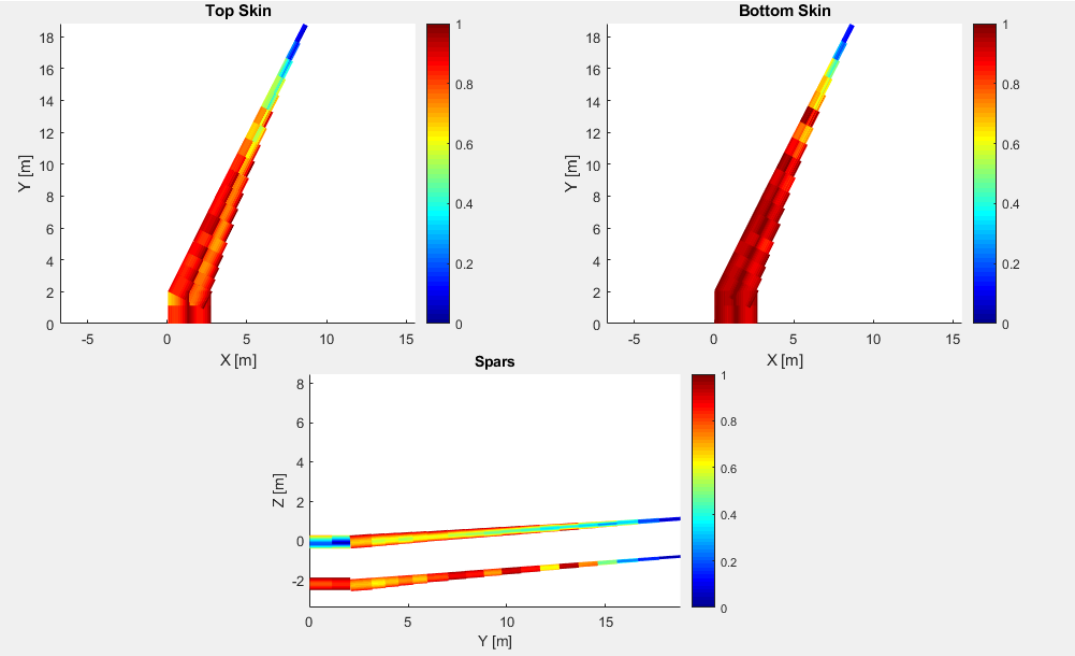

(b) Strain index -loadcase 2

Figure 5.6: Strain index for the different loadcases used in PRTOEUS for design D1.

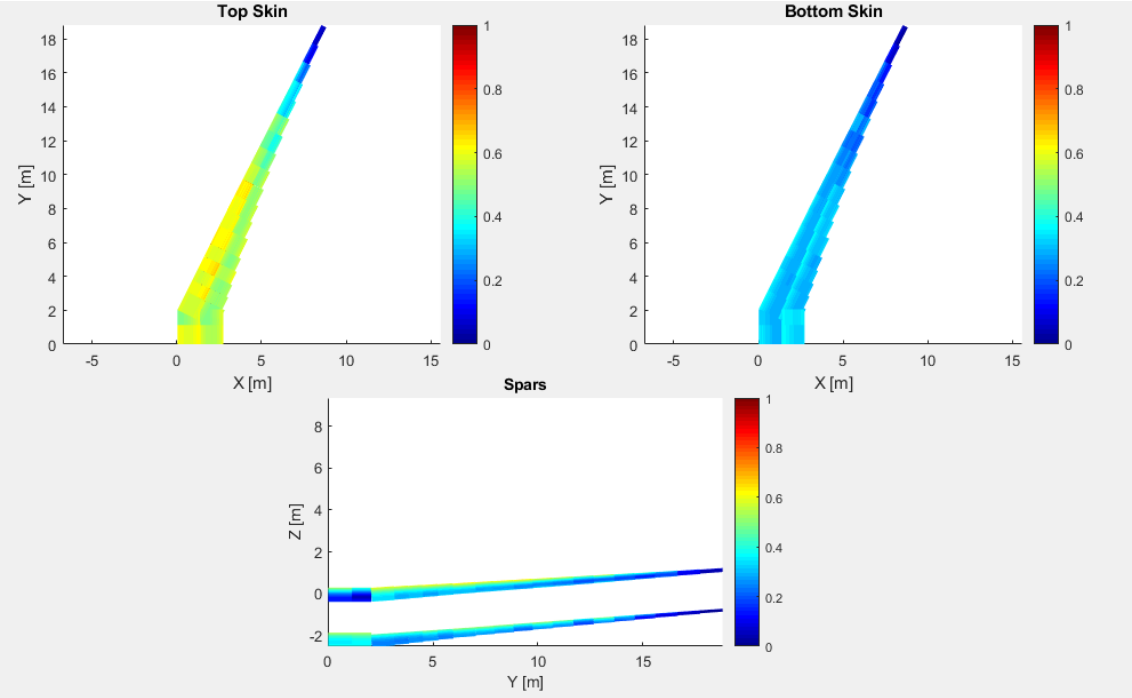

(a) Strain index -loadcase 3

Figure 5.7: Strain index for the different loadcases used in PRTOEUS for design D1.(**contd)

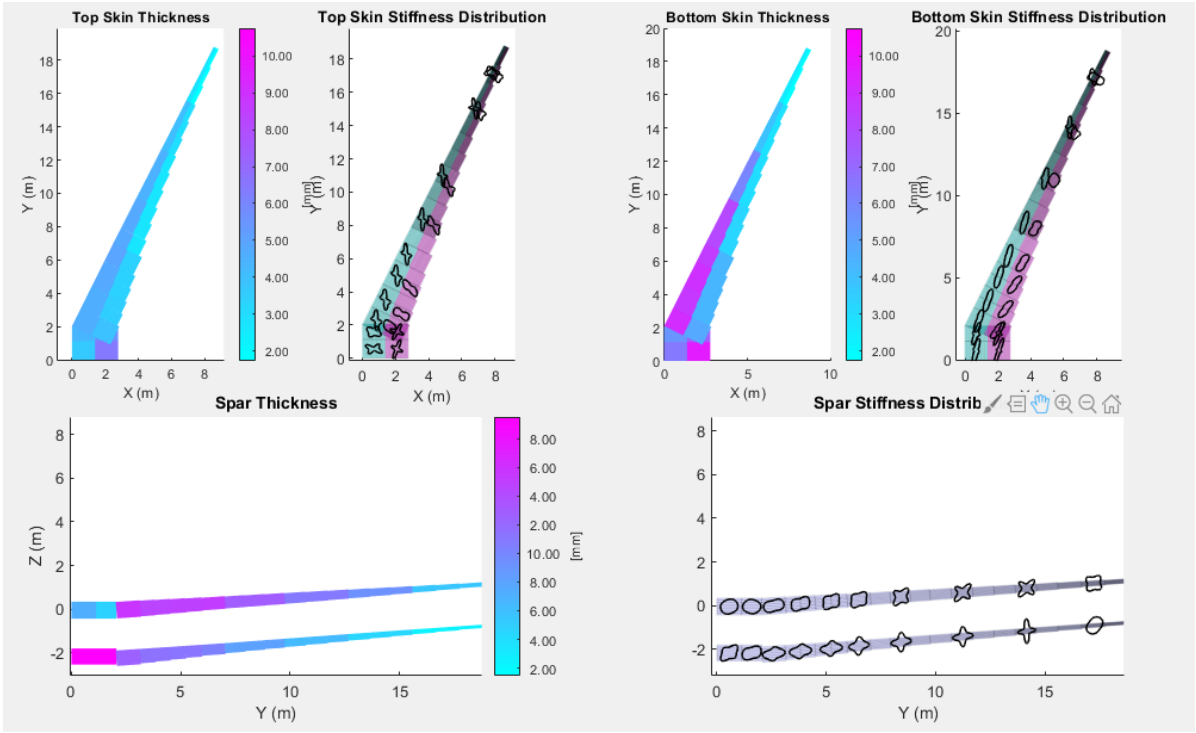

(a) In-plane stiffness and thickness in design D1.

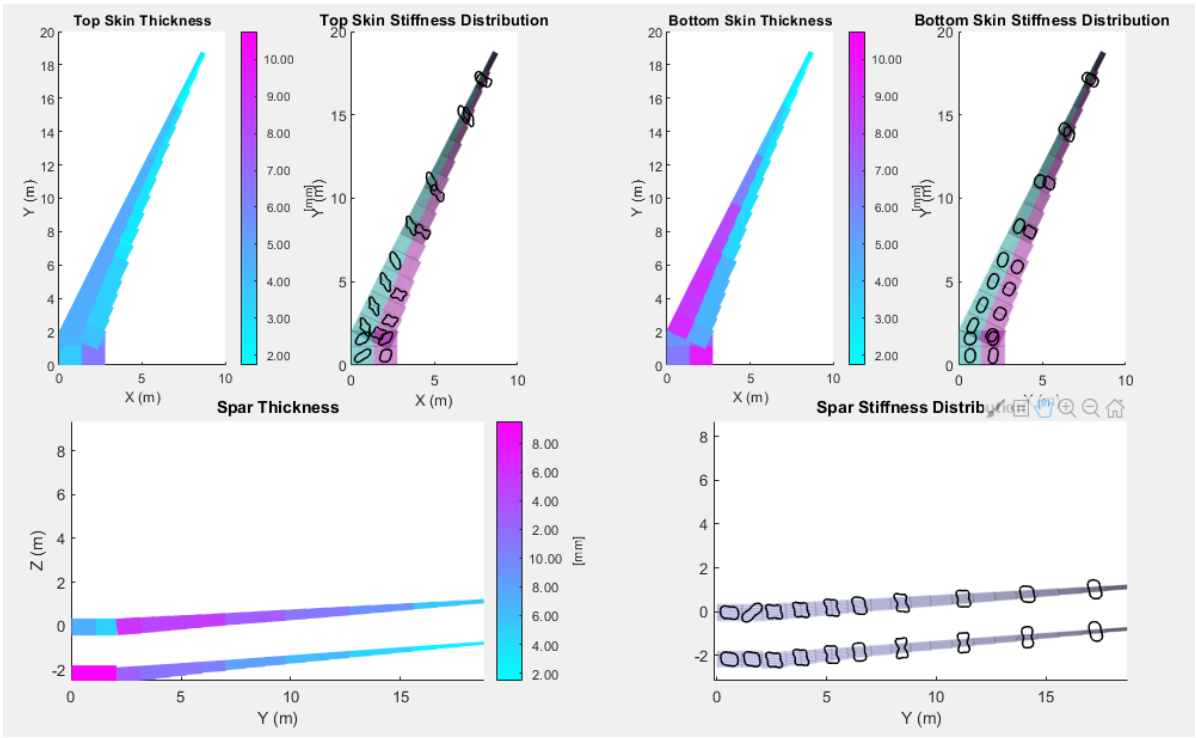

(b) In-plane stiffness and thickness in design D2.

Figure 5.8: In-plane and out-plane stiffness for design D1.

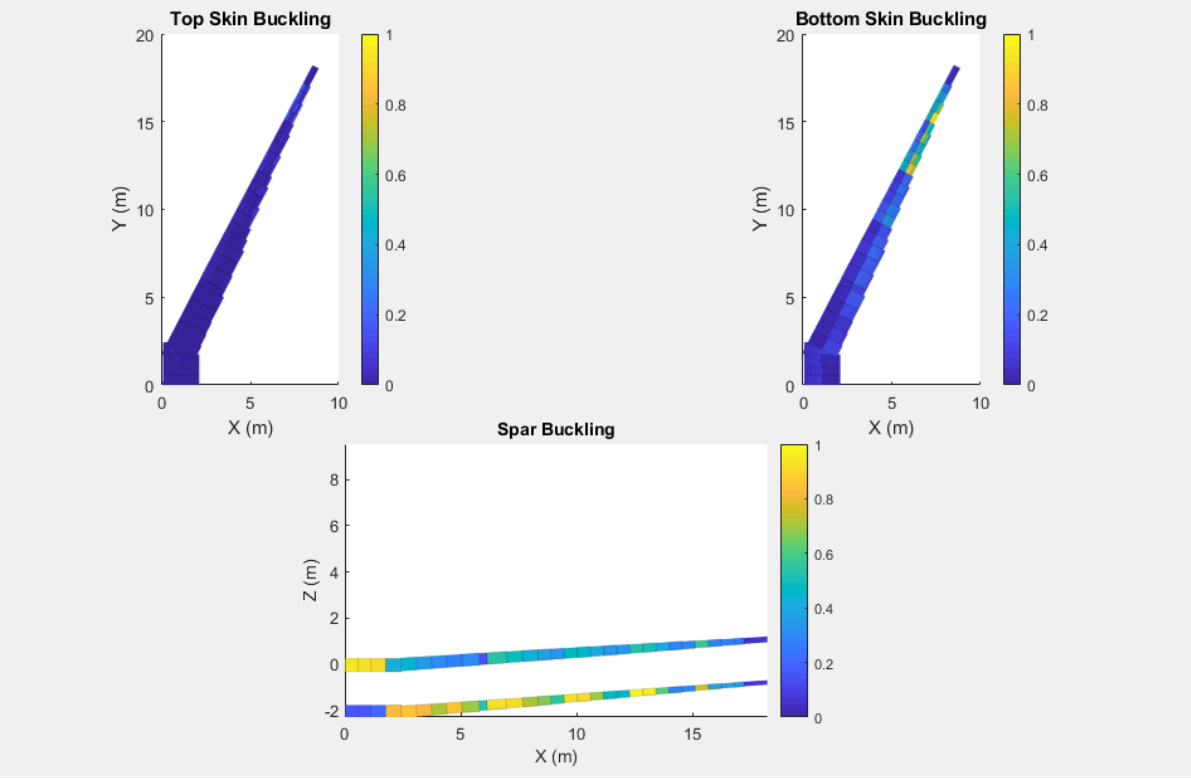

(a) Metal based design sensitivities

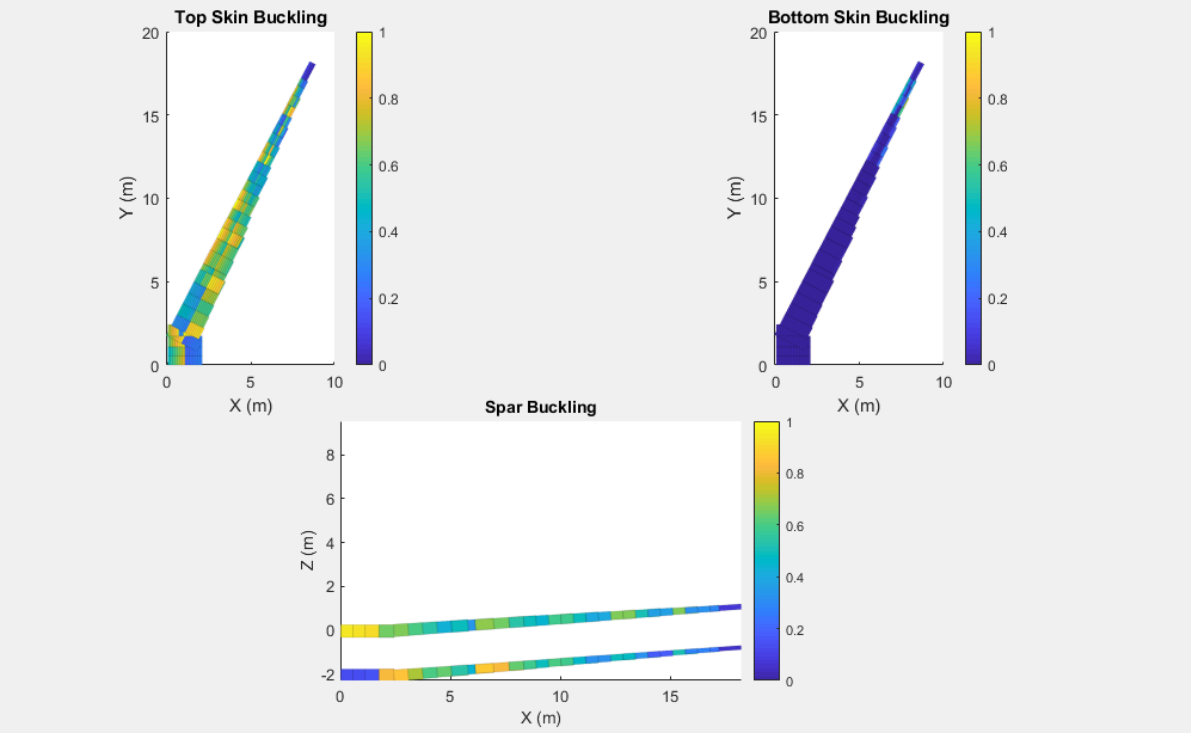

(b) Composite based design sensitivities

Figure 5.9: Buckling index for different loadcases obtained using PROTEUS for design D2.

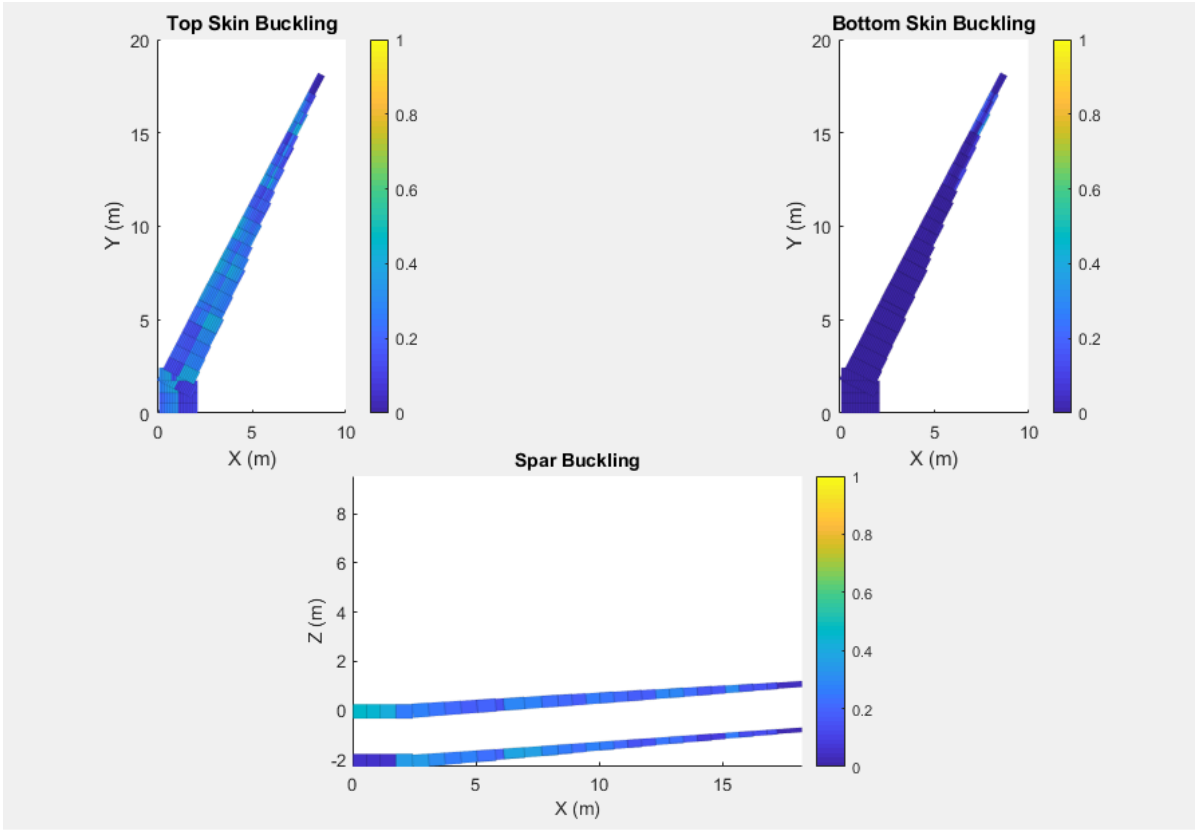

(a) Composite based design sensitivities

Figure 5.10: Buckling index for different loadcases obtained using PROTEUS for design D2.(**contd)

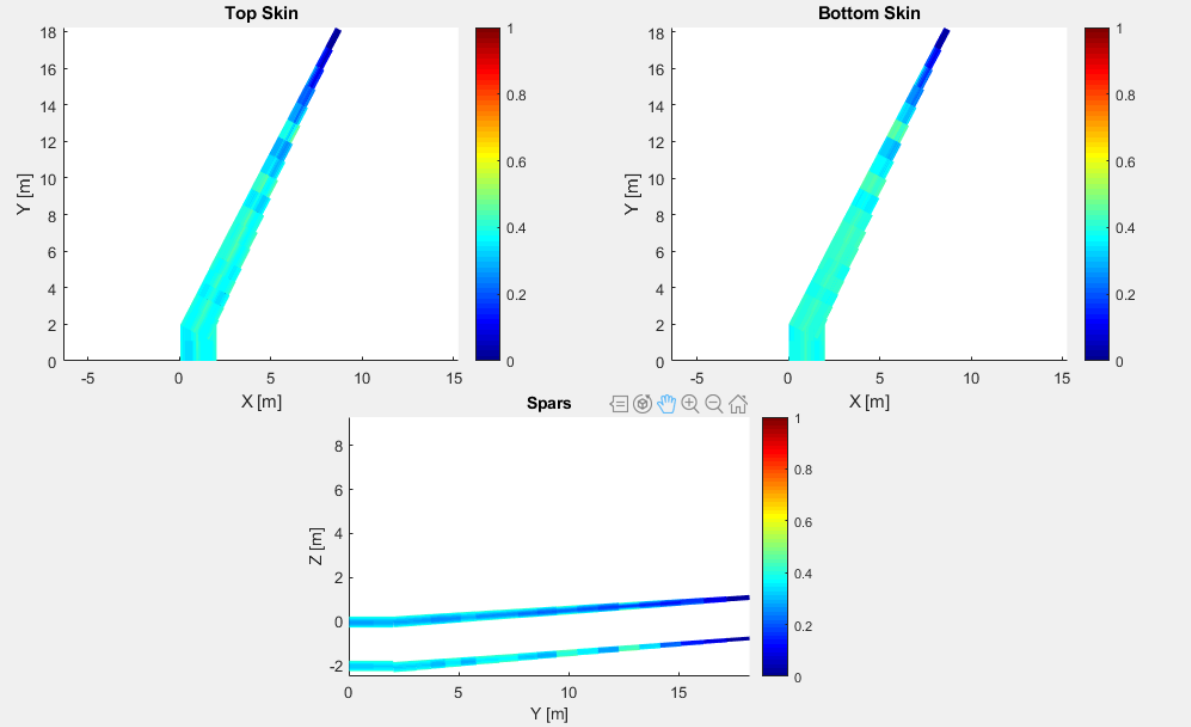

(a) strain index - LC1

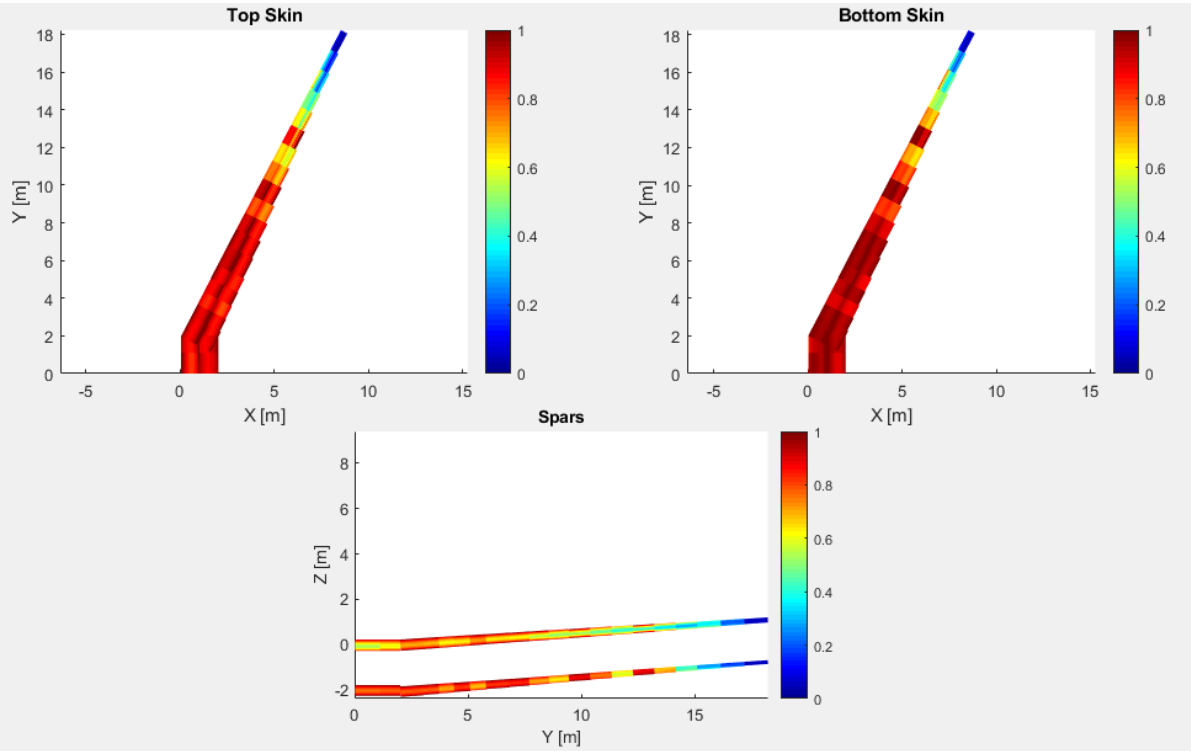

(b) strain index - LC2

Figure 5.11: Strain index for different loadcases obtained using PROTEUS for design D2.

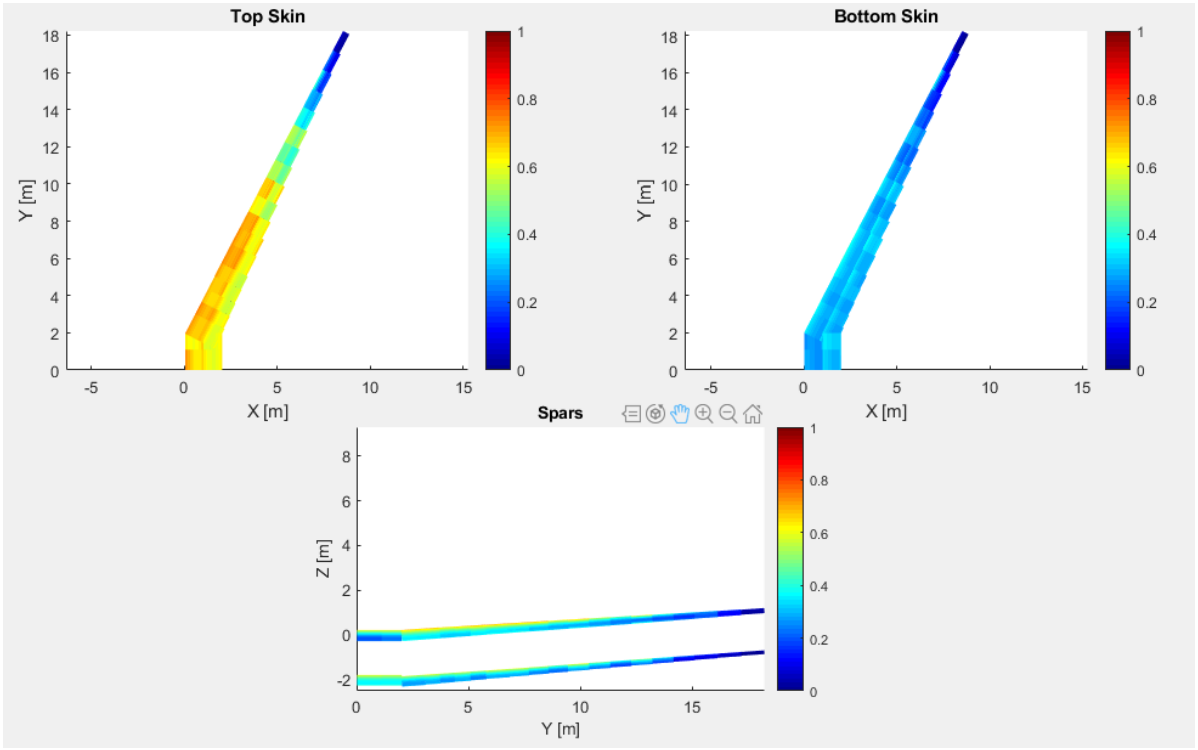

(a) strain index - LC3

Figure 5.12: Strain index for different loadcases obtained using PROTEUS for design D2.(**contd)

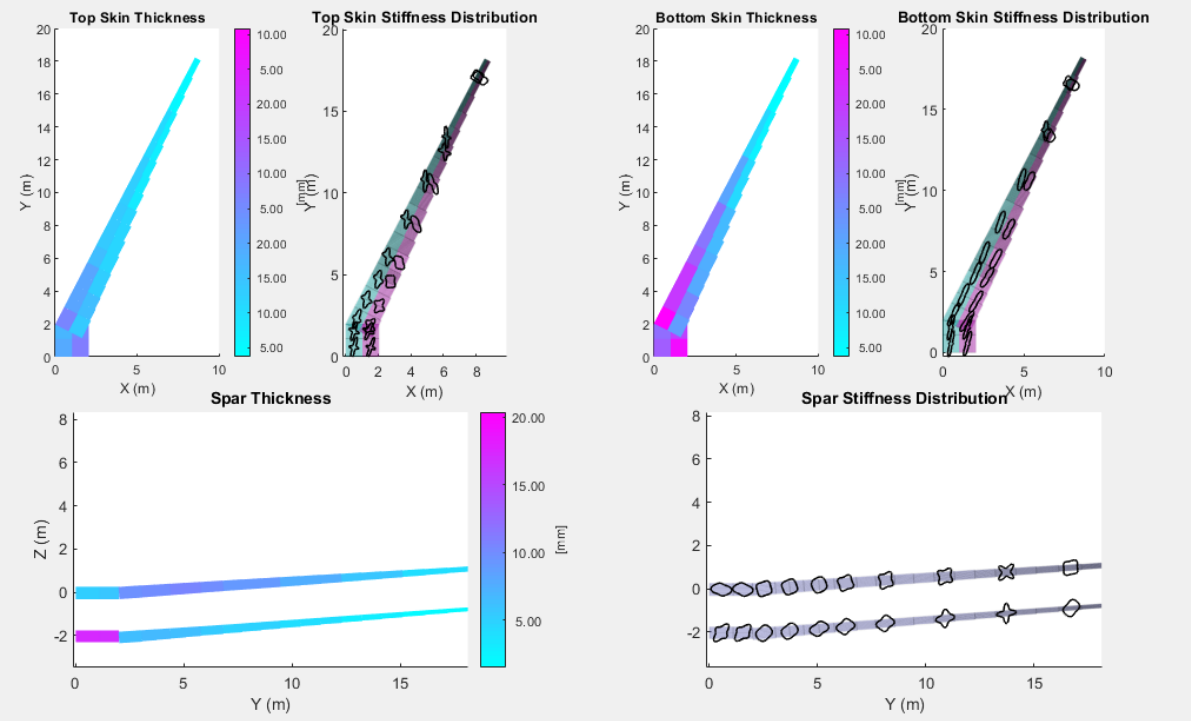

(a) In-plane stiffness and thickness

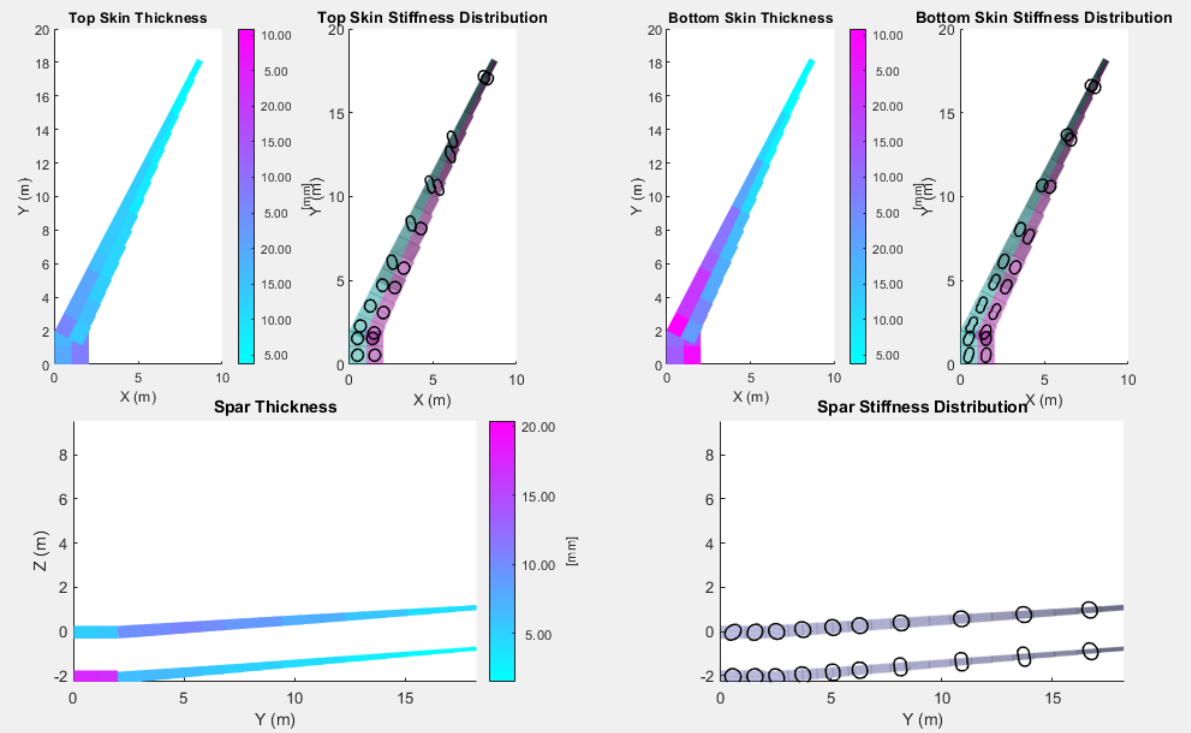

(b) Out-plane stiffness and thickness

Figure 5.13: Stiffness and thickness for design D2.

6

Conclusions and recommendations

The work presented in the current thesis leads towards the answers sought for the research questions developed in the literature study. The results are divided into two major sections, one of KADMOS functionality and the other of applying the functionality in the design of composite wing which forms the design study. These are used to make the conclusions and recommendations.

1. The difficulty of using PROTEUS as a tool in optimization studies was established earlier. A surrogate modeling methodology was thus successfully developed as an addition to the KADMOS functions in order to overcome the computational barrier. The key difficulty found in applying the surrogate modeling methodology was the selection of an appropriate set of functions from all the functions. These could then be combined to reduce the computational cost evaluated based on run time and the number of runs to be made. Four algorithms are developed for this purpose among which the adjacency based algorithm proved to have the highest accuracy and performance requirement. The kriging method is used to model the training data. After the surrogate model was obtained validation tests were conducted. The validation study indicated the surrogate model accuracy compared to the original PROTEUS tool for various design points.

2. Using the surrogate modeling methodology design studies were carried out for the PROTEUS based design while the metal (EMWET) based design was created through the traditional optimization. With the final superimposition of PROTEUS optimization on the intermediate planform designs the final wing designs D1 and D2 are obtained. The wing optimized composite designs D1 and D2 display similarities in the distribution of laminates. This is attributed to the similar buckling and strain response obtained in the two scenarios. The majority of the fuel weight reduction thus occurs from the inclusion of PROTEUS in the optimization workflow to obtain a more efficient intermediate planform design in terms of planform design variables(length, aspect ratio, λ_1 and λ_2).

3. The difference in the fuel efficiency for the two designs indicates a reduction in fuel weight for the wing designed using PROTEUS surrogate methodology. The surrogate methodology thus gives a better design in terms of fuel efficiency.

Some recommendations can also be listed which present additional studies which can be done.

1. The functionality of creating a surrogate of tool in an MDO study, in KADMOS, can be extended to different tools other than PROTEUS. This is due to the nature of KADMOS being a common platform to formulate an MDO problem. In order to be able to extend the methodology an understanding of the factors causing errors is needed. These errors are caused by the physics based tool being replaced by the surrogate based tool. There is hence an uncertainty in the final design due to these error factors. An evaluation of the uncertainty caused due to the error in surrogate model can be a possible future study.

2. In the current study, the kriging method was used for modeling the training data with respect to the design variables. Further studies could hence be done in regards to the differences caused in

the accuracy due to the various estimated models which can be generated. The artificial neural network and radial basis functions present two such possible estimation models.

3. The design using the surrogate method presented an advantage in fuel consumption. While the reduction in fuel is useful, an extra computational effort of building the surrogate model is required. One possible line of questioning here would be if the computational cost is lower than the reduction in fuel costs which can be accumulated over the lifetime o the aircraft.

4. The MDO problem itself can be made more representative of real aircraft design through the inclusion of the PHALANX flight dynamics tool which is already a part the repository of TU Delft. The tool can be used to evaluate the dynamic flight responses as well include constraints for situations such as engine failure on take-off and crosswinds.

7

Appendix-A

The interaction between openLEGO and KADMOS has been something attempted for the first time. In order for future researchers to know firsthand some preliminary knowledge, some o the steps taken up in the setting up of the complete workflow have been mentioned in the current appendix.

Certain values from the files required for the KADMOS file have to modify it. These are attributes other than uID which are necessary to run the tools and were previously not compatible with the working of openLEGO and openMDAO.

- In case of the point list the attribute $\mathbf{maptype} = '\mathbf{vector}'$ is required to denote the vector input in case of the point list required for the aerofoil profiles.
- The description of the wing needs to be done using **symmetry** attribute, which describes the plane about the which the wing is similarly generated as the original wing.
- The **mode** description n of the tools included in the CMDOWS file need to be used to create separate function files based on the names of the $function\ name + tool$.
- instances of the variables occurring the inputs and outputs need to added in the variable names to make sure circular couplings can be included in the final MDO workflow.

8

Appendix-B

Code to modify the variable complexity problem to obtain increased feed forward coupling in the KAD-MOS graph. The various representative MDO problems were used as test cases for verification.

```
# Import modules
import random


def modify_fpg(fpg, n_disciplines, function_order, feedback_ratio):
    """
    :param fpg: Fundamental problem graph
    :param n_disciplines: Number of function nodes
   :param function_order: Sequence of the function within the Fundamental problem graph
     :param feedback_ratio: Give the ratio between the number of feed-
forward and feedback coupling nodes
    (value x : 1 < x < infinity)
    :return:
    """
    # add the variables in the coupling
    coupling_nodes_dictionary = fpg.get_coupling_nodes_dict()

    function_nodes = fpg.get_function_nodes()
    function_nodes.remove('F')
    function_nodes.remove('G01')
    if n_disciplines > 8:
     coupled_functions = fpg.graph['problem_formulation']['function_ordering']
        ['coupled']
        for function_idx1 in coupled_functions:

            function_idx1_index = function_order.index(function_idx1)
            print(function_idx1_index)
            function_outputs = fpg.get_targets(function_idx1)

            for function_idx2 in function_nodes:
                function_idx2_index = function_order.index(function_idx2)
                if function_idx2_index < function_idx1_index:
                    removal_edges = []
                    addition_edges = []
```

```
                    # Find if couplings exist between the two elements
                    try:
                num_coupling_nodes = len(coupling_nodes_dictionary[function_idx1]
                        [function_idx2])
                    except:
                        num_coupling_nodes = 0

                    # if couplings exist
                    if num_coupling_nodes > 0:
                couplings = coupling_nodes_dictionary[function_idx1][function_idx2]
                        print (len(couplings))
                        random_coupling_value =
                 random.randint(1, int(len(couplings) / feedback_ratio) + 1)
                sample = random.sample(list(couplings), random_coupling_value)

                        for coupling in couplings:
                            removal_edges.append((coupling, function_idx2))

                        fpg.remove_edges_from(removal_edges)

                        for sample_element in sample:
                         addition_edges.append((sample_element, function_idx2))
                            fpg.add_edges_from(addition_edges)

                else:
                    removal_edges = []
                    addition_edges = []

                    if not function_idx1 == function_idx2:
                        try:
                   num_coupling_nodes = len(coupling_nodes_dictionary[function_idx1]
                                [function_idx2])
                        except:
                            num_coupling_nodes = 0

                        if num_coupling_nodes > 0:
                           couplings = coupling_nodes_dictionary[function_idx1]
                                [function_idx2]
                      random_coupling_value = random.randint(1, len(function_outputs))
                                sample = random.sample(list(function_outputs)
                                , random_coupling_value)



                                for coupling in couplings:
                                removal_edges.append((coupling, function_idx2))

                                fpg.remove_edges_from(removal_edges)

                                for sample_element in sample:
                             addition_edges.append((sample_element, function_idx2))
                                fpg.add_edges_from(addition_edges)

    else:
        for function_idx1 in function_nodes:
            for function_idx2 in function_nodes:
```

```
                removal_edges = []
                addition_edges = []

                if function_idx1 < function_idx2:
                    try:
                num_coupling_nodes = len(coupling_nodes_dictionary[function_idx1]
                        [function_idx2])
                    except:
                        num_coupling_nodes = 0

                    if num_coupling_nodes > 0:
                couplings = coupling_nodes_dictionary[function_idx1][function_idx2]
                        random_coupling_value =
                  random.randint(1, int(len(couplings/feedback_ratio)) + 1)
                sample = random.sample(list(couplings), random_coupling_value)

                        # print(sample)

                        for coupling in couplings:
                            removal_edges.append((coupling, function_idx2))

                        fpg.remove_edges_from(removal_edges)

                        for sample_element in sample:
                     addition_edges.append((sample_element, function_idx2))
                        fpg.add_edges_from(addition_edges)

    return fpg
```

Bibliography

[1] MS Windows NT kernel description. https://commons.wikimedia.org/wiki/File:Graph_example_(Graph_theory).png. Accessed: 2010-09-30.

[2] Benedikt Aigner, Imco van Gent, Gianfranco La Rocca, Eike Stumpf, and Leo LM Veldhuis. Graph-based algorithms and data-driven documents for formulation and visualization of large mdo systems. *CEAS Aeronautical Journal*, 9(4):695–709, 2018.

[3] Timothy R Brooks, Graeme Kennedy, and Joaquim Martins. High-fidelity multipoint aerostructural optimization of a high aspect ratio tow-steered composite wing. In *58th AIAA/ASCE/AHS/ASC Structures, Structural Dynamics, and Materials Conference*, page 1350, 2017.

[4] Kinga Budziak. *Aerodynamic Analysis with Athena Vortex Lattice (AVL)*. Hamburg: Aircraft Design and Systems Group (AERO), Department of Automotive …, 2015.

[5] Kazuhisa Chiba, Shigeru Obayashi, Kazuhiro Nakahashi, and Hiroyuki Morino. High-fidelity multidisciplinary design optimization of wing shape for regional jet aircraft. In *International Conference on Evolutionary Multi-Criterion Optimization*, pages 621–635. Springer, 2005.

[6] Pier Davide Ciampa and Björn Nagel. Towards the 3rd generation mdo collaborative environment. ICAS, 2016.

[7] Pier Davide Ciampa and Björn Nagel. The agile paradigm: the next generation of collaborative mdo. In *18th AIAA/ISSMO Multidisciplinary Analysis and Optimization Conference*, page 4137, 2017.

[8] Pier Davide Ciampa, Erwin Moerland, Doreen Seider, Erik Baalbergen, Riccardo Lombardi, and Roberto D'Ippolito. A collaborative architecture supporting agile design of complex aeronautics products. In *18th AIAA/ISSMO Multidisciplinary Analysis and Optimization Conference*, page 4138, 2017.

[9] D de Vries. *Towards the Industrialization of MDAO*. PhD thesis, Master's thesis, Delft University of Technology, 2017.

[10] Daniël de Vries, I van Gent, G la Rocca, and S Binder. Openlego demonstration: A link between agile and openmdao. In *First European OpenMDAO workshop*, 2017.

[11] Olivier de Weck, Jeremy Agte, Jaroslaw Sobieszczanski-Sobieski, Paul Arendsen, Alan Morris, and Martin Spieck. State-of-the-art and future trends in multidisciplinary design optimization. In *48th Aiaa/Asme/Asce/Ahs/Asc Structures, Structural Dynamics, and Materials Conference*, page 1905, 2007.

[12] Adam Diedrich, James Hileman, David Tan, Karen Willcox, and Zoltan Spakovszky. Multidisciplinary design and optimization of the silent aircraft. In *44th AIAA aerospace sciences meeting and exhibit*, page 1323, 2006.

[13] Johannes Dillinger. *Static aeroelastic optimization of composite wings with variable stiffness laminates*. PhD thesis, DLR-German Aerospace Center, 2015.

[14] Mark Drela. Xfoil: An analysis and design system for low reynolds number airfoils. In *Low Reynolds number aerodynamics*, pages 1–12. Springer, 1989.

[15] FE Eastep, VA Tischler, VB Venkayya, and NS Khot. Aeroelastic tailoring of composite structures. *Journal of aircraft*, 36(6):1041–1047, 1999.

[16] Ali Elham and Michel van Tooren. Beyond quasi-analytical methods for preliminary structural sizing and weight estimation of lifting surfaces. In *56th AIAA/ASCE/AHS/ASC Structures, Structural Dynamics, and Materials Conference*, page 0399, 2015.

[17] Ali Elham and Michel JL van Tooren. Tool for preliminary structural sizing, weight estimation, and aeroelastic optimization of lifting surfaces. *Proceedings of the Institution of Mechanical Engineers, Part G: Journal of Aerospace Engineering*, 230(2):280–295, 2016.

[18] RJM Elmendorp, Roelof Vos, and Gianfranco La Rocca. A conceptual design and analysis method for conventional and unconventional airplanes. In *ICAS 2014: Proceedings of the 29th Congress of the International Council of the Aeronautical Sciences, St. Petersburg, Russia, 7-12 September 2014*. International Council of Aeronautical Sciences, 2014.

[19] Alexander IJ Forrester and Andy J Keane. Recent advances in surrogate-based optimization. *Progress in aerospace sciences*, 45(1-3):50–79, 2009.

[20] PR Garabedian and DG Korn. Analysis of transonic airfoils. *Communications on Pure and Applied Mathematics*, 24(6):841–851, 1971.

[21] Frank H Gern, Amir H Naghshineh-Pour, Erwin Sulaeman, Rakesh K Kapania, and Raphael T Haftka. Structural wing sizing for multidisciplinary design optimization of a strut-braced wing. *Journal of aircraft*, 38(1):154–163, 2001.

[22] Tushar Goel, Raphael T Haftka, Wei Shyy, and Nestor V Queipo. Ensemble of surrogates. *Structural and Multidisciplinary Optimization*, 33(3):199–216, 2007.

[23] Justin S. Gray. *Design Optimization of a Boundary Layer Ingestion Propulsor Using a Coupled Aeropropulsive Model*. PhD thesis, University of Michigan, 2018.

[24] Justin S. Gray, John T. Hwang, Joaquim R. R. A. Martins, Kenneth T. Moore, and Bret A. Naylor. OpenMDAO: An open-source framework for multidisciplinary design, analysis, and optimization. *Structural and Multidisciplinary Optimization*, 59(4):1075–1104, April 2019. doi: 10.1007/s00158-019-02211-z.

[25] Justin S. Gray, John T. Hwang, Joaquim R. R. A. Martins, Kenneth T. Moore, and Bret A. Naylor. OpenMDAO: An Open-Source Framework for Multidisciplinary Design, Analysis, and Optimization. *Structural and Multidisciplinary Optimization*, 59:1075–1104, 2019. doi: 10.1007/s00158-019-02211-z.

[26] David R Greatrix. *Powered Flight*. Springer, 2012.

[27] Xiangyu Gu, Arthur Rizzi, and Eike Stumpf. Application of computational aerodynamic analysis and optimization in a multi-fidelity distributed overall aircraft design system. Technical report, Lehrstuhl und Institut für Luft-und Raumfahrtsysteme (ILR), 2017.

[28] Xiangyu Gu, Pier Davide Ciampa, and Björn Nagel. An automated cfd analysis workflow in overall aircraft design applications. *CEAS Aeronautical Journal*, 9(1):3–13, 2018.

[29] Aric A. Hagberg, Daniel A. Schult, and Pieter J. Swart. Exploring network structure, dynamics, and function using networkx. In Gaël Varoquaux, Travis Vaught, and Jarrod Millman, editors, *Proceedings of the 7th Python in Science Conference*, pages 11 – 15, Pasadena, CA USA, 2008.

[30] Zhong-Hua Han and Ke-Shi Zhang. Surrogate-based optimization. In *Real-world applications of genetic algorithms*. InTech, 2012.

[31] Eric S. Hendricks. *A multi-level multi-design point approach for gas turbine cycle and turbine conceptual design*. PhD thesis, Georgia Institute of Technology, 2017.

[32] Michael Chamberlain Henson et al. *Optimization of Aircraft Tow Steered Composite Wing Structures*. PhD thesis, 2018.

[33] John T Hwang and Andrew Ning. Large-scale multidisciplinary optimization of an electric aircraft for on-demand mobility. In *2018 AIAA/ASCE/AHS/ASC Structures, Structural Dynamics, and Materials Conference*, page 1384, 2018.

[34] L Jaeger, Christian Gogu, Stéphane Segonds, and Christian Bes. Aircraft multidisciplinary design optimization under both model and design variables uncertainty. *Journal of Aircraft*, 50(2):528–538, 2013.

[35] Anya Jones, Karen Willcox, and James Hileman. Distributed multidisciplinary optimization of aircraft design and takeoff operations for low noise. In *48th AIAA/ASME/ASCE/AHS/ASC Structures, Structural Dynamics, and Materials Conference*, page 1856, 2006.

[36] Christine Jutte and Bret K Stanford. Aeroelastic tailoring of transport aircraft wings: State-of-the-art and potential enabling technologies. 2014.

[37] Masahiro Kanazaki, Kentaro Tanaka, Shinkyu Jeong, and Kazuomi Yamamoto. Multi-objective aerodynamic optimization of elements' setting for high-lift airfoil using kriging model. In *44th AIAA Aerospace Sciences Meeting and Exhibit*, page 1471, 2006.

[38] Graeme Kennedy and Joaquim Martins. A comparison of metallic and composite aircraft wings using aerostructural design optimization. In *12th AIAA Aviation Technology, Integration, and Operations (ATIO) Conference and 14th AIAA/ISSMO Multidisciplinary Analysis and Optimization Conference*, page 5475, 2012.

[39] Donald E Knuth and Jayme L Szwarcfiter. A structured program to generate all topological sorting arrangements. *Information Processing Letters*, 2(6):153–157, 1974.

[40] Takayasu Kumano, Shinkyu Jeong, Shigeru Obayashi, Yasushi Ito, Keita Hatanaka, and Hiroyuki Morino. Multidisciplinary design optimization of wing shape for a small jet aircraft using kriging model. In *44th AIAA Aerospace Sciences Meeting and Exhibit*, page 932, 2006.

[41] Andrew Lambe, Graeme Kennedy, and Joaquim Martins. Multidisciplinary design optimization of an aircraft wing via a matrix-free approach. In *15th AIAA/ISSMO Multidisciplinary Analysis and Optimization Conference*, page 2429, 2014.

[42] AC Lambers. Development of surrogate-based multidisciplinary optimization methodology with flutter constraints for aircraft conceptual design. 2016.

[43] Leifur Thor Leifsson. *Multidisciplinary design optimization of low-noise transport aircraft*. PhD thesis, Virginia Tech, 2005.

[44] Jun Luo, Lan Huang, Mark Hachey, and Ram Tiwari. Adjacency method for finding connected subsets of a graph: An application of graph theory to spatial statistics. *Communications in Statistics-Simulation and Computation*, 38(5):1136–1151, 2009.

[45] J Mariens, A Elham, and MJL Van Tooren. Quasi-three-dimensional aerodynamic solver for multidisciplinary design optimization of lifting surfaces. *Journal of Aircraft*, 51(2):547–558, 2014.

[46] Joaquim RRA Martins and John T Hwang. Review and unification of methods for computing derivatives of multidisciplinary computational models. *AIAA journal*, 51(11):2582–2599, 2013.

[47] Joaquim RRA Martins and Andrew B Lambe. Multidisciplinary design optimization: a survey of architectures. *AIAA journal*, 51(9):2049–2075, 2013.

[48] Michael D McKay. Latin hypercube sampling as a tool in uncertainty analysis of computer models. In *Proceedings of the 24th conference on Winter simulation*, pages 557–564, 1992.

[49] Craig C Morris. *Flight dynamic constraints in conceptual aircraft multidisciplinary analysis and design optimization*. PhD thesis, Virginia Tech, 2014.

[50] Björn Nagel, Daniel Böhnke, Volker Gollnick, Peter Schmollgruber, Arthur Rizzi, Gianfranco La Rocca, and Juan J Alonso. Communication in aircraft design: Can we establish a common language. In *28th International Congress of the Aeronautical Sciences*, pages 1–13, 2012.

[51] Ed Obert. *Aerodynamic design of transport aircraft*. IOS press, 2009.

[52] Athanasios Papageorgiou, Mehdi Tarkian, Kristian Amadori, and Johan Ölvander. Multidisciplinary optimization of unmanned aircraft considering radar signature, sensors, and trajectory constraints. *Journal of Aircraft*, 55(4):1629–1640, 2018.

[53] David J Pate, Justin Gray, and Brian J German. A graph theoretic approach to problem formulation for multidisciplinary design analysis and optimization. *Structural and Multidisciplinary Optimization*, 49(5):743–760, 2014.

[54] Ryan Peoples and Karen Willcox. Value-based multidisciplinary optimization for commercial aircraft design and business risk assessment. *Journal of Aircraft*, 43(4):913–921, 2006.

[55] Ruben Perez, Hugh Liu, and Kamran Behdinan. Flight dynamics and control multidisciplinary integration in aircraft conceptual design optimization. In *10th AIAA/ISSMO Multidisciplinary Analysis and Optimization Conference*, page 4435, 2004.

[56] Ruben E Perez, Hugh HT Liu, and Kamran Behdinan. Multidisciplinary optimization framework for control-configuration integration in aircraft conceptual design. *Journal of Aircraft*, 43(6):1937–1948, 2006.

[57] Till Pfeiffer, Björn Nagel, Daniel Böhnke, Arthur Rizzi, and Mark Voskuijl. Implementation of a heterogeneous, variable-fidelity framework for flight mechanics analysis in preliminary aircraft design. In *60th German Aerospace Congress (DLRK)*, 2011.

[58] Nestor V. Queipo, Raphael T. Haftka, Wei Shyy, Tushar Goel, Rajkumar Vaidyanathan, and P. Kevin Tucker. Surrogate-based analysis and optimization. *Progress in Aerospace Sciences*, 41(1):1 – 28, 2005. ISSN 0376-0421. doi: https://doi.org/10.1016/j.paerosci.2005.02.001. URL http://www.sciencedirect.com/science/article/pii/S0376042105000102.

[59] Nestor V Queipo, Raphael T Haftka, Wei Shyy, Tushar Goel, Rajkumar Vaidyanathan, and P Kevin Tucker. Surrogate-based analysis and optimization. *Progress in aerospace sciences*, 41(1):1–28, 2005.

[60] CS Rao, HM Tsai, and T Ray. Aircraft configuration design using a multidisciplinary optimization approach. In *42nd AIAA Aerospace Sciences Meeting and Exhibit*, page 536, 2004.

[61] Arthur Rizzi, Mengmeng Zhang, Bjoern Nagel, Daniel Boehnke, and Pierre Saquet. Towards a unified framework using cpacs for geometry management in aircraft design. In *50th AIAA Aerospace Sciences Meeting including the New Horizons Forum and Aerospace Exposition*, page 549, 2012.

[62] Jan Roskam. *Airplane Design: Part 6-Preliminary Calculation of Aerodynamic, Thrust and Power Characteristics*. DARcorporation, 1985.

[63] Ulrich Schumann. On the effect of emissions from aircraft engines on the state of the atmosphere. In *Annales Geophysicae*, pages 365–384, 1994.

[64] R Sellar, S Batill, and J Renaud. Response surface based, concurrent subspace optimization for multidisciplinary system design. In *34th aerospace sciences meeting and exhibit*, page 714, 1996.

[65] Michael H Shirk, Terrence J Hertz, and Terrence A Weisshaar. Aeroelastic tailoring-theory, practice, and promise. *Journal of Aircraft*, 23(1):6–18, 1986.

[66] Richard B Skoog and Harvey H Brown. A method for the determination of the spanwise load distribution of a flexible swept wing at subsonic speeds. 1951.

[67] J. Sobieszczanski-Sobieski and R. T. Haftka. Multidisciplinary aerospace design optimization: survey of recent developments. *Structural optimization*, 14(1):1–23, Aug 1997. ISSN 1615-1488. doi: 10.1007/BF01197554. URL https://doi.org/10.1007/BF01197554.

[68] Jaroslaw Sobieszczanski-Sobieski, Alan Morris, and Michel van Tooren. *Multidisciplinary design optimization supported by knowledge based engineering*. John Wiley & Sons, 2015.

[69] O Stodieck, JE Cooper, PM Weaver, and P Kealy. Aeroelastic tailoring of a representative wing box using tow-steered composites. *AIAA journal*, pages 1425–1439, 2016.

[70] A Striz and W Lee. Multidisciplinary optimization of a transport aircraft wing. In *5th Symposium on Multidisciplinary Analysis and Optimization*, page 4410, 1994.

[71] Afzal Suleman, Fernando Lau, Jose Vale, and Frederico Afonso. Multidisciplinary performance based optimization of morphing aircraft. In *22nd AIAA/ASME/AHS Adaptive Structures Conference*, page 0761, 2014.

[72] Nathan Tedford and Joaquim Martins. On the common structure of mdo problems: a comparison of architectures. In *11th AIAA/ISSMO Multidisciplinary Analysis and Optimization Conference*, page 7080, 2006.

[73] T Tzong, G Sikes, and M Loikkanen. Multidisciplinary design optimization of a large transport aircraft wing. In *Aerospace Design Conference*, page 1002, 1992.

[74] A van der Wees, J Van Muijden, and J Van der Vooren. A fast robust viscous-inviscid interaction solver for transonic flowabout wing/body configurations on the basis of full potential theory. In *23rd Fluid Dynamics, Plasmadynamics, and Lasers Conference*, page 3026, 1993.

[75] Imco van Gent, Pier Davide Ciampa, Benedikt Aigner, Jonas Jepsen, Gianfranco La Rocca, and Joost Schut. Knowledge architecture supporting collaborative mdo in the agile paradigm. In *18th AIAA/ISSMO Multidisciplinary Analysis and Optimization Conference*, page 4139, 2017.

[76] Imco van Gent, Gianfranco La Rocca, and Maurice Hoogreef. Cmdows: A proposed new standard to store and exchange mdo systems. 10 2017.

[77] Imco van Gent, Gianfranco La Rocca, and Leo L Veldhuis. Composing mdao symphonies: graph-based generation and manipulation of large multidisciplinary systems. In *18th AIAA/ISSMO Multidisciplinary Analysis and Optimization Conference*, page 3663, 2017.

[78] G Gary Wang and Songqing Shan. Review of metamodeling techniques in support of engineering design optimization. *Journal of Mechanical design*, 129(4):370–380, 2007.

[79] Terrence A Weisshaar. Aeroelastic tailoring of forward swept composite wings. *Journal of Aircraft*, 18(8):669–676, 1981.

[80] NPM Werter and R De Breuker. A novel dynamic aeroelastic framework for aeroelastic tailoring and structural optimisation. *Composite Structures*, 158:369–386, 2016.

[81] Brett Wujek, John Renaud, Stephen Batill, Eric Johnson, and Jay Brockman. Design flow management and multidisciplinary design optimization in application to aircraft concept sizing. In *34th Aerospace Sciences Meeting and Exhibit*, page 713, 1996.

[82] Tobias Wunderlich, Sascha Dähne, Lars Heinrich, and Lars Reimer. Multidisciplinary optimization of an nlf forward swept wing in combination with aeroelastic tailoring using cfrp. *CEAS Aeronautical Journal*, 8(4):673–690, 2017.

[83] Tobias F Wunderlich. Multidisciplinary wing design and optimization for transport aircraft. *DLR, September*, 22, 2008.

[84] Raul Yondo, Esther Andrés, and Eusebio Valero. A review on design of experiments and surrogate models in aircraft real-time and many-query aerodynamic analyses. *Progress in Aerospace Sciences*, 2017.

[85] Yang Yu, Zhengjie Wang, and Shijun Guo. Efficient method for aeroelastic tailoring of composite wing to minimize gust response. *International Journal of Aerospace Engineering*, 2017, 2017.

[86] Ke-shi Zhang, Zhong-hua Han, Wei-ji Li, and Wen-ping Song. Coupled aerodynamic/structural optimization of a subsonic transport wing using a surrogate model. *Journal of Aircraft*, 45(6): 2167–2171, 2008.